

Physics/Computational Issues for Transport Analysis of QPS devices (DELTA5D vs. DKES)

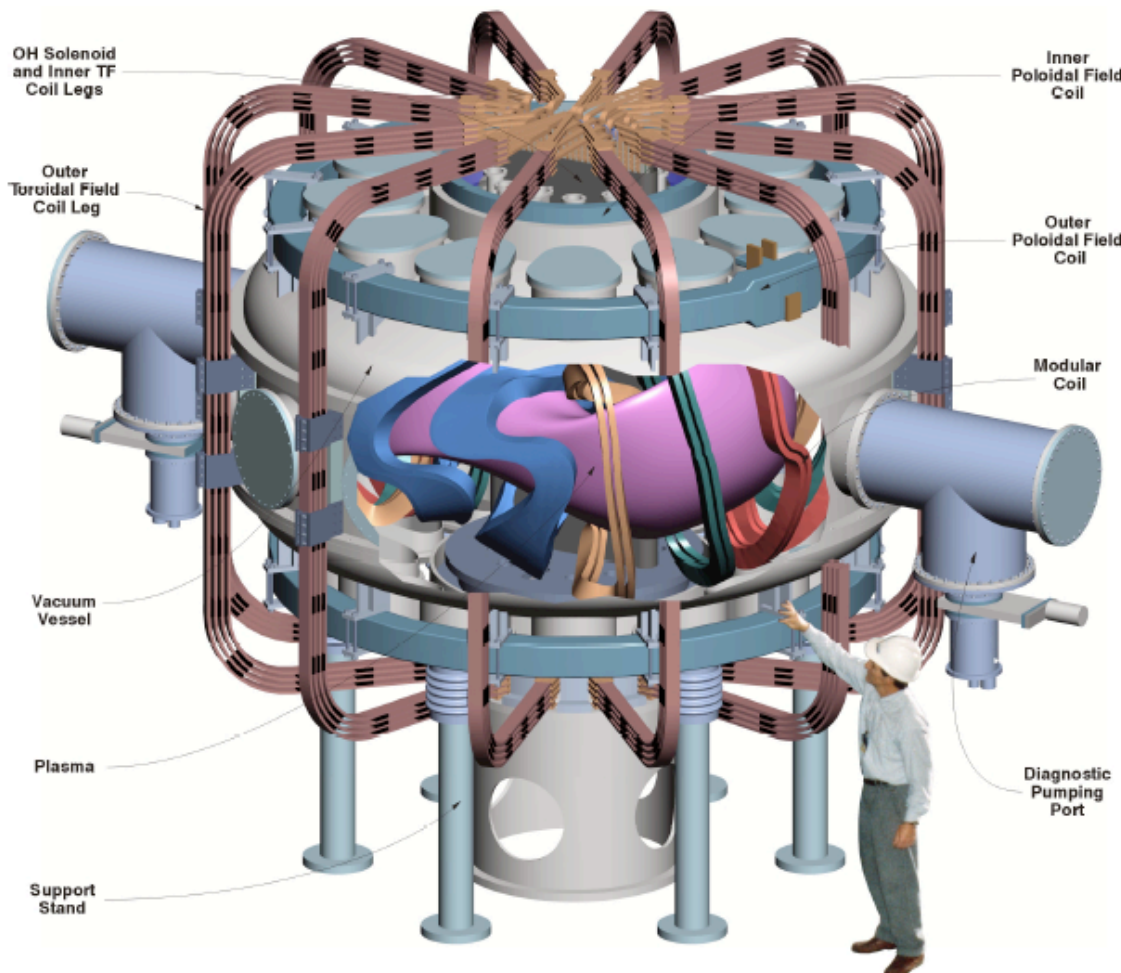
D.A. Spong

*Oak Ridge National Laboratory, P.O. Box 2009, Oak Ridge, TN
37831-8073*

*in collaboration with Steve Hirshman, Jim Lyon, Lee Berry, Dave
Mikkelsen, Mike Zarnstorff*

**Kinetic Theory Workshop 2002
Greifswald, Germany, Oct. 21 - 23**

QPS is a very low aspect ratio ($A = 2.7$) Quasi-poloidal stellarator



- $\langle R_0 \rangle = 0.9 \text{ m}$, $\langle a \rangle = 0.33 \text{ m}$, $\langle B \rangle = 1 \text{ T} \pm 0.2 \text{ T}$ for 1sec, $I_p \sqcup 150 \text{ kA}$, $P_{ECH} = 0.6\text{-}1.2 \text{ Mw}$, $P_{ICH} = 1\text{-}3 \text{ Mw}$
- This experiment will test:
 - Equilibrium robustness
 - Neoclassical and anomalous transport
 - Stability limits up to $\langle \beta \rangle = 2.5\%$
 - Bootstrap current effects
 - Reduced poloidal viscosity effects on shear flow transport reduction
 - Configurational flexibility

Our transport analysis has focused on optimization targets and comparisons between configurations

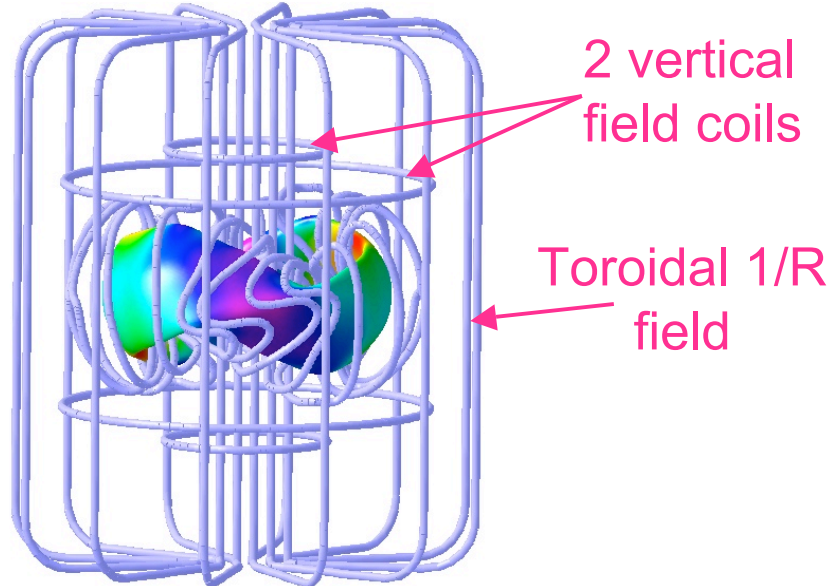
Optimization Strategy

- QOS optimizations (1996 - 1999)
 - J^* , J , B_{\min} , B_{\max}
 - DKES
- QPS optimizations (2000 - present)
 - β_{eff}
 - Poloidal symmetry
 - DKES

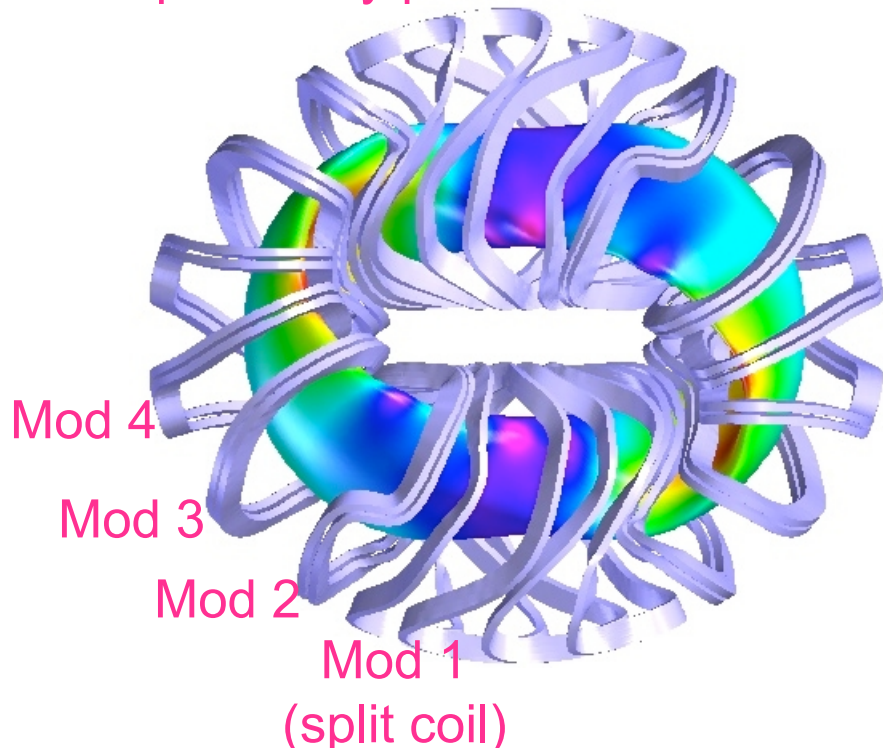
Evaluation Tools

- NEO β_{eff} , Poloidal symmetry
- DKES
 - Setup, mode selection
 - Parallel runs
 - Energy integration
- DELTA5D Monte Carlo
 - Global full-f model
 - ICRF heating
 - NBI heating efficiency
 - Alpha losses
 - Bootstrap current
- 1-1/2 D model

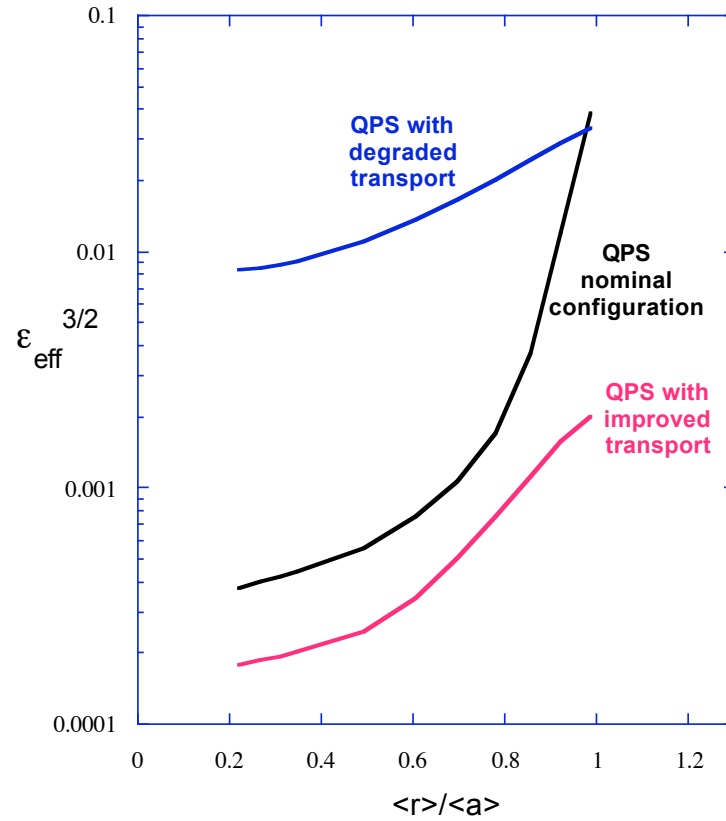
However, with the QPS configuration becoming fixed, we are shifting over to flexibility studies and transport predictions.



4 independently powered modular coils



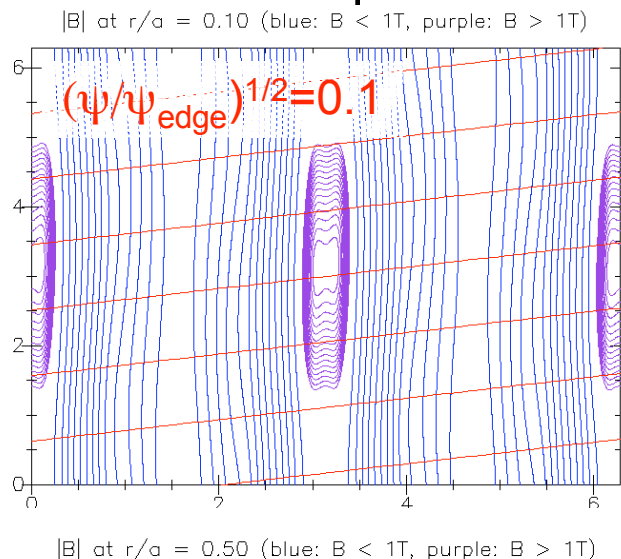
QPS Flexibility Studies



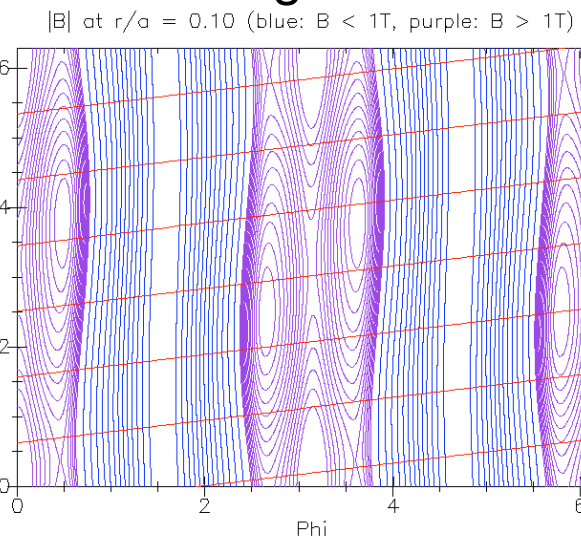
- Modular coil currents can vary $\pm 25\%$
- Vertical field currents can vary ± 100 kA
- Toroidal field currents can vary ± 70 kA

QPS Flexibility Studies - effect on $|B|$

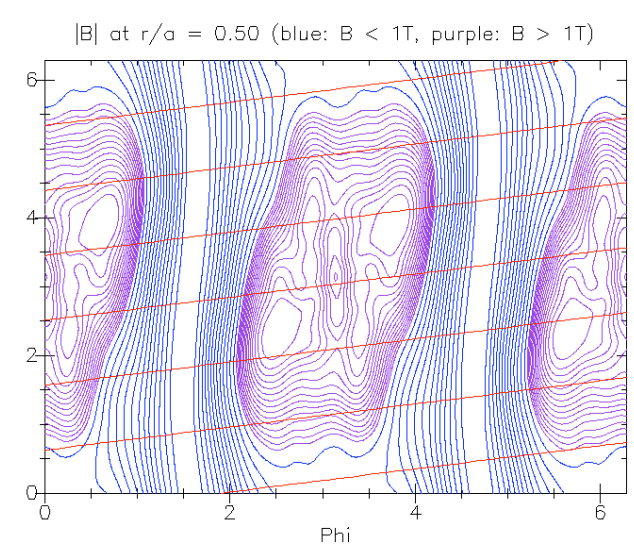
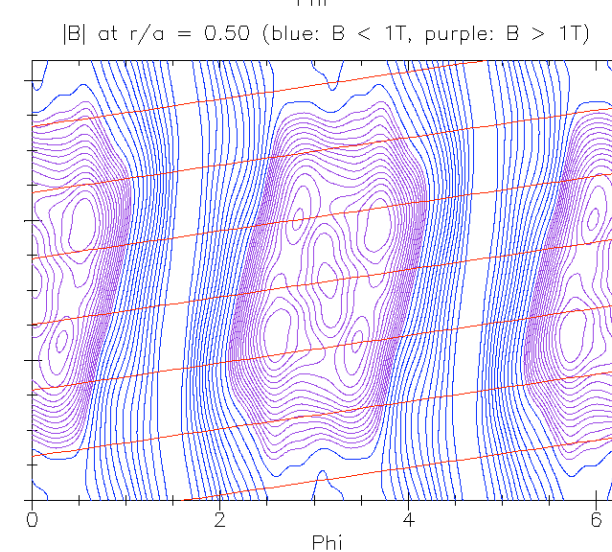
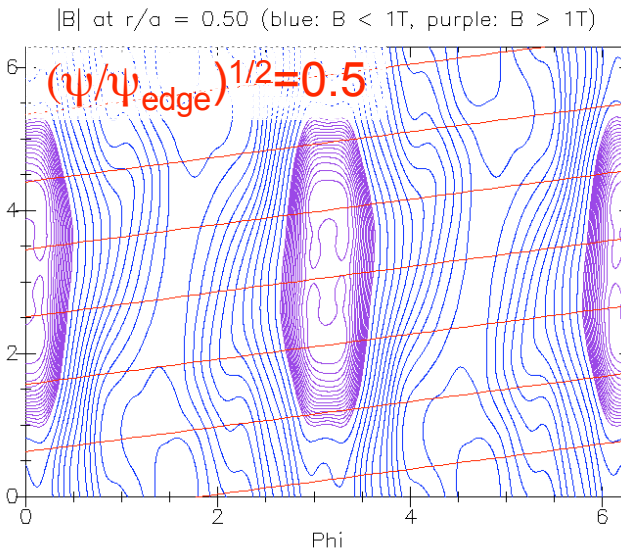
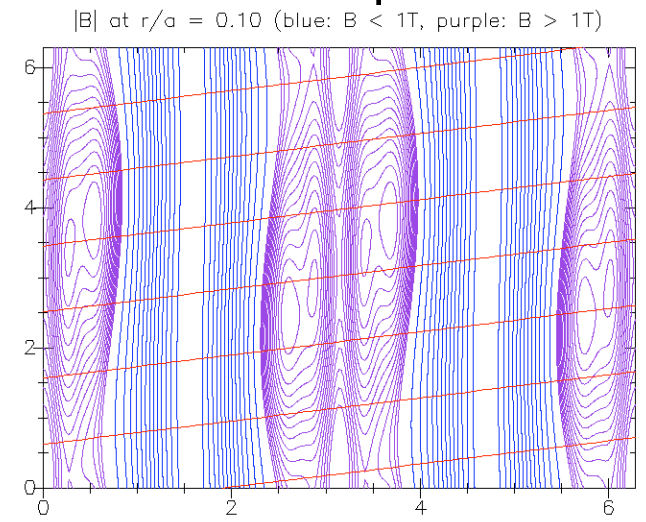
Degraded transport



Nominal configuration



Improved transport



The DKES (Drift Kinetic Equation Solver) provides the full neoclassical transport coefficient matrix (multi-helicity)

$$I_i = \frac{1}{T} \bar{Q} \cdot \vec{B}_s = \sum_{j=1}^3 L_{ij} A_j$$

$$A_j = \begin{bmatrix} n & \frac{3}{2} \frac{T}{T} e E_r \\ n & \frac{T}{T} \\ e & \langle \vec{E} \cdot \vec{B} \rangle \\ T & \langle B^2 \rangle \end{bmatrix}$$

$$L_{ij} = n \frac{2}{\sqrt{\pi}} \int_0^\infty dK \sqrt{K} e^{-K} g_i g_j D_{ij}$$

where $g_1 = g_3 = 1$, $g_2 = K$, $K = \frac{v}{v_{th}}$

$$D_{11} = D_{12} = D_{21} = D_{22} = \frac{v_{th}}{2} \frac{B v_{th}}{dr} \frac{d}{dr} \frac{1}{K} \frac{1}{\sqrt{K}} D_{11}$$

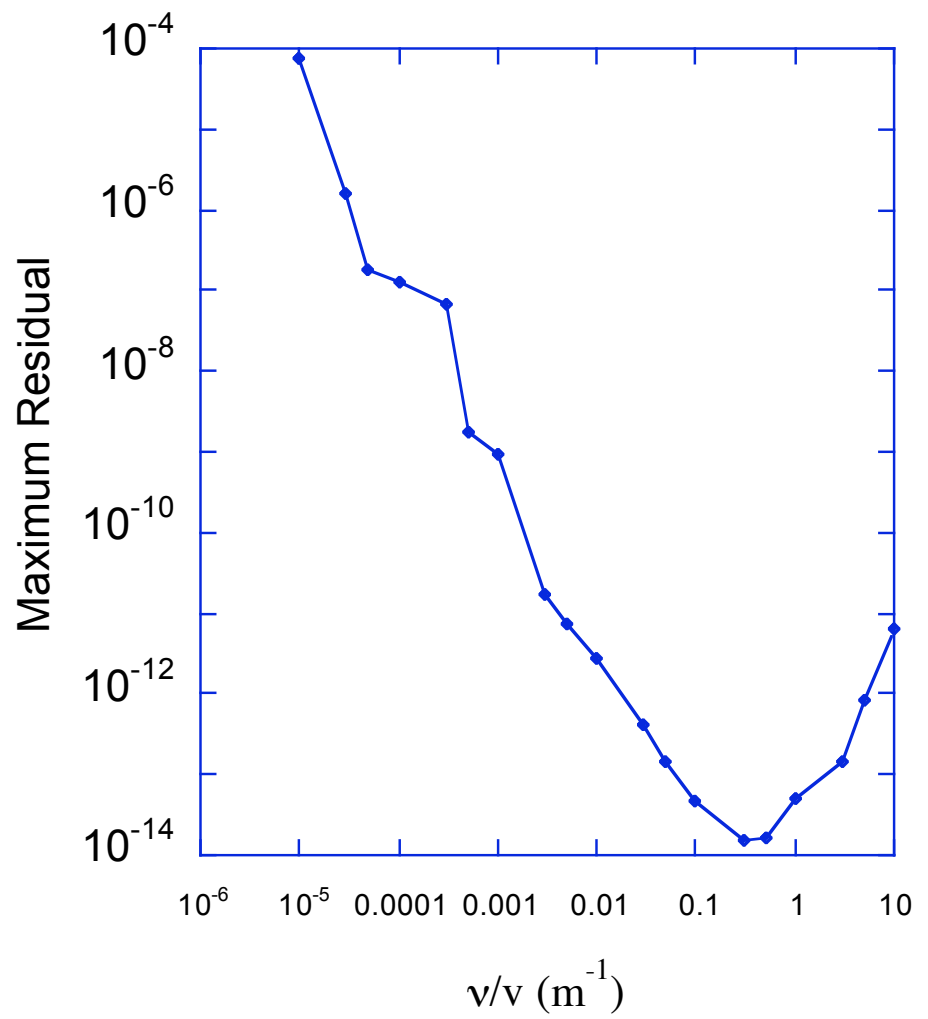
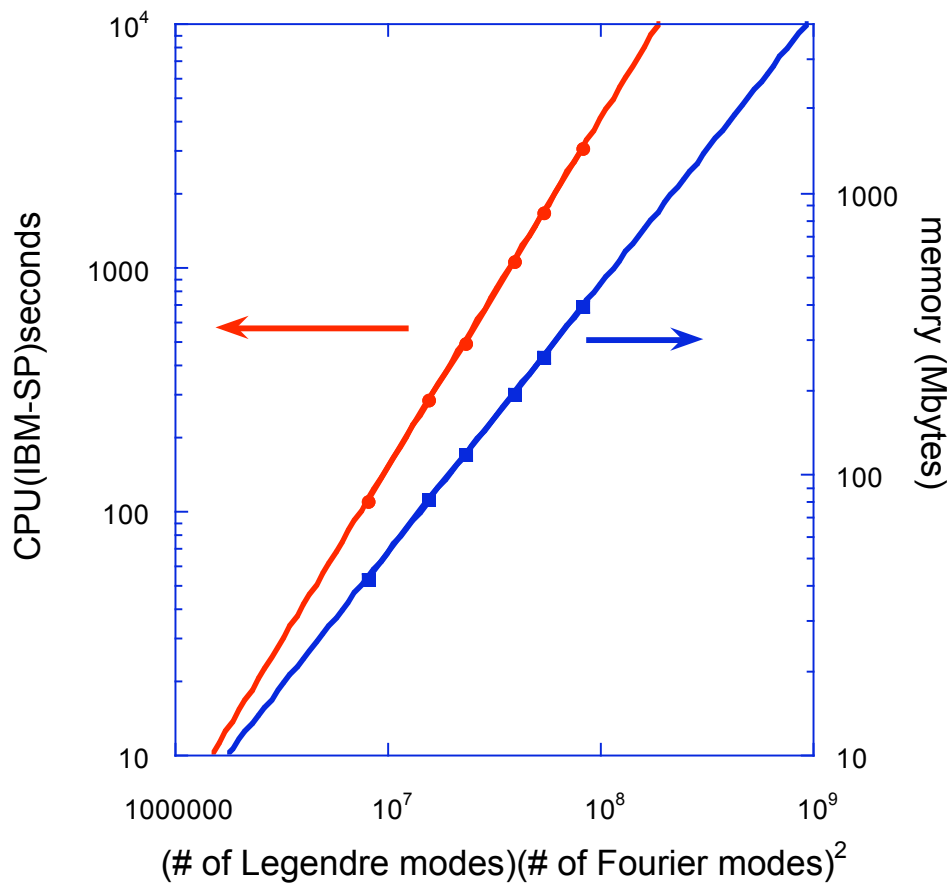
$$D_{31} = D_{32} = D_{13} = D_{23} = \frac{v_{th}}{2} \frac{B v_{th}}{dr} \frac{d}{dr} \frac{1}{K} D_{31}$$

$$D_{33} = \frac{v_{th}}{2} \sqrt{K} D_{33}$$

$$D_{ij} = D_{ij} \frac{1}{v}, \frac{E_r}{v}$$

(i.e., to carry out the above integrals, one will need to generate a 2-D matrix of D 's vs. these parameters for each flux surface)

DKES performance, memory and residuals limitations



DKES transport dependencies show that both $L_{11} \propto \sqrt{\mu}$ and $L_{11} \propto 1/\mu$ regimes are accessed.

These ranges are based on the maximum n, T in the profile, $e\mu/kT(a) = 1$, and looking from thermal energy to 9 times thermal (as sampled by velocity integrals for μ)

- ECH electrons:

$$7 \times 10^{-5} < \mu/v < 10^{-3}$$

$$8 \times 10^{-5} < E/v < 2 \times 10^{-4}$$

- ECH ions:

$$6 \times 10^{-3} < \mu/v < 7 \times 10^{-2}$$

$$10^{-2} < E/v < 3 \times 10^{-2}$$

- ICH electrons:

$$3 \times 10^{-3} < \mu/v < 4 \times 10^{-2}$$

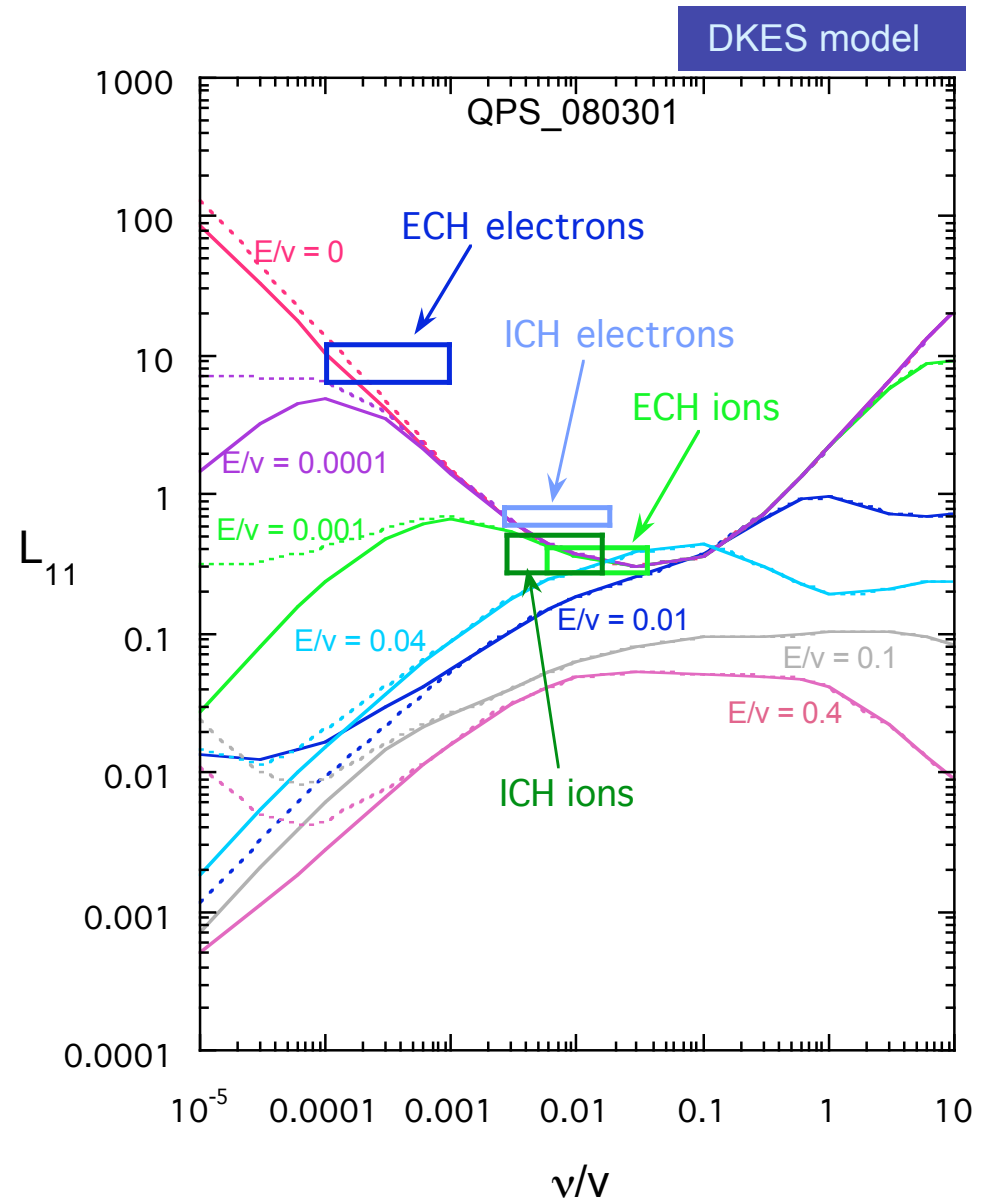
$$5 \times 10^{-5} < E/v < 2 \times 10^{-4}$$

- ICH ions:

$$2 \times 10^{-3} < \mu/v < 3 \times 10^{-2}$$

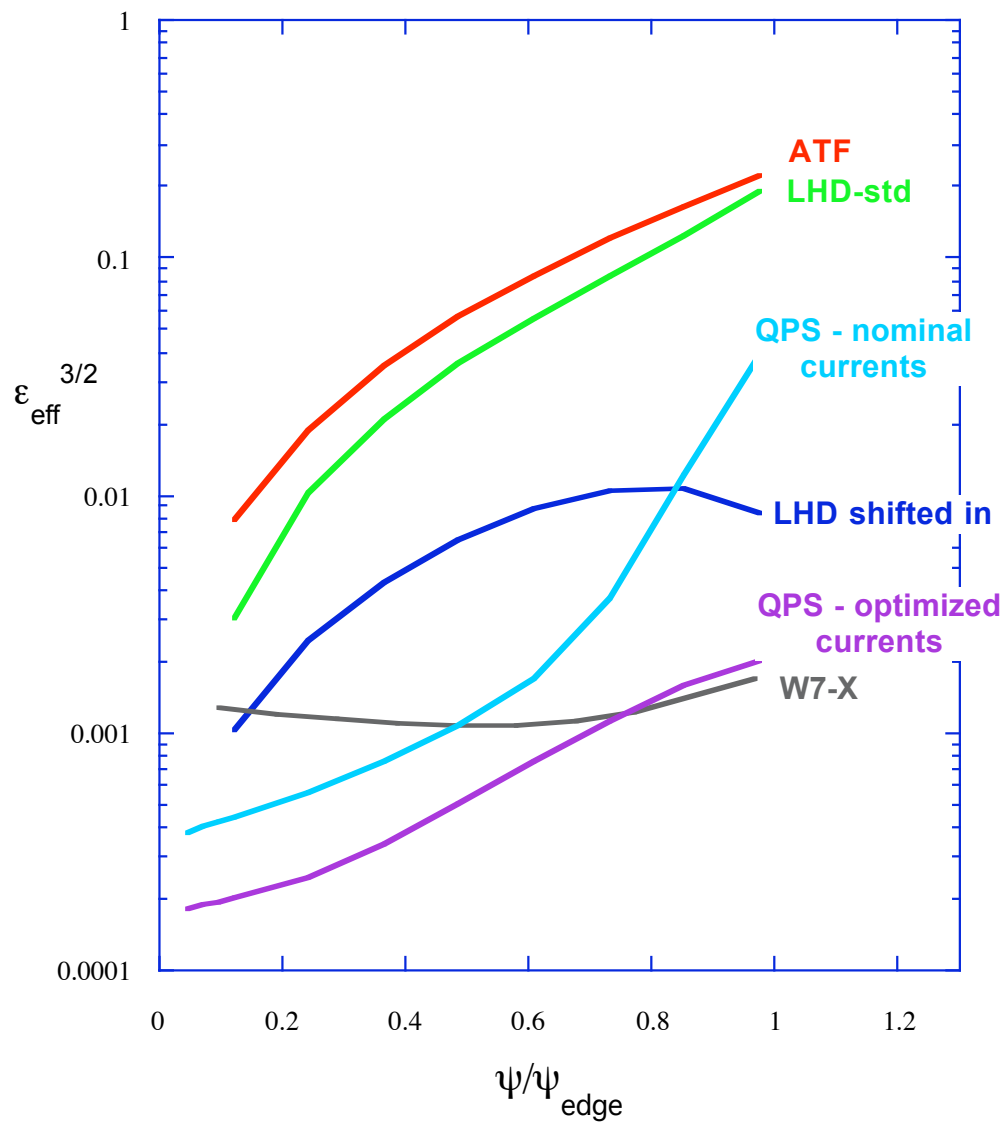
$$2 \times 10^{-3} < E/v < 6 \times 10^{-3}$$

Note: these L11's are based on the gb4 device.

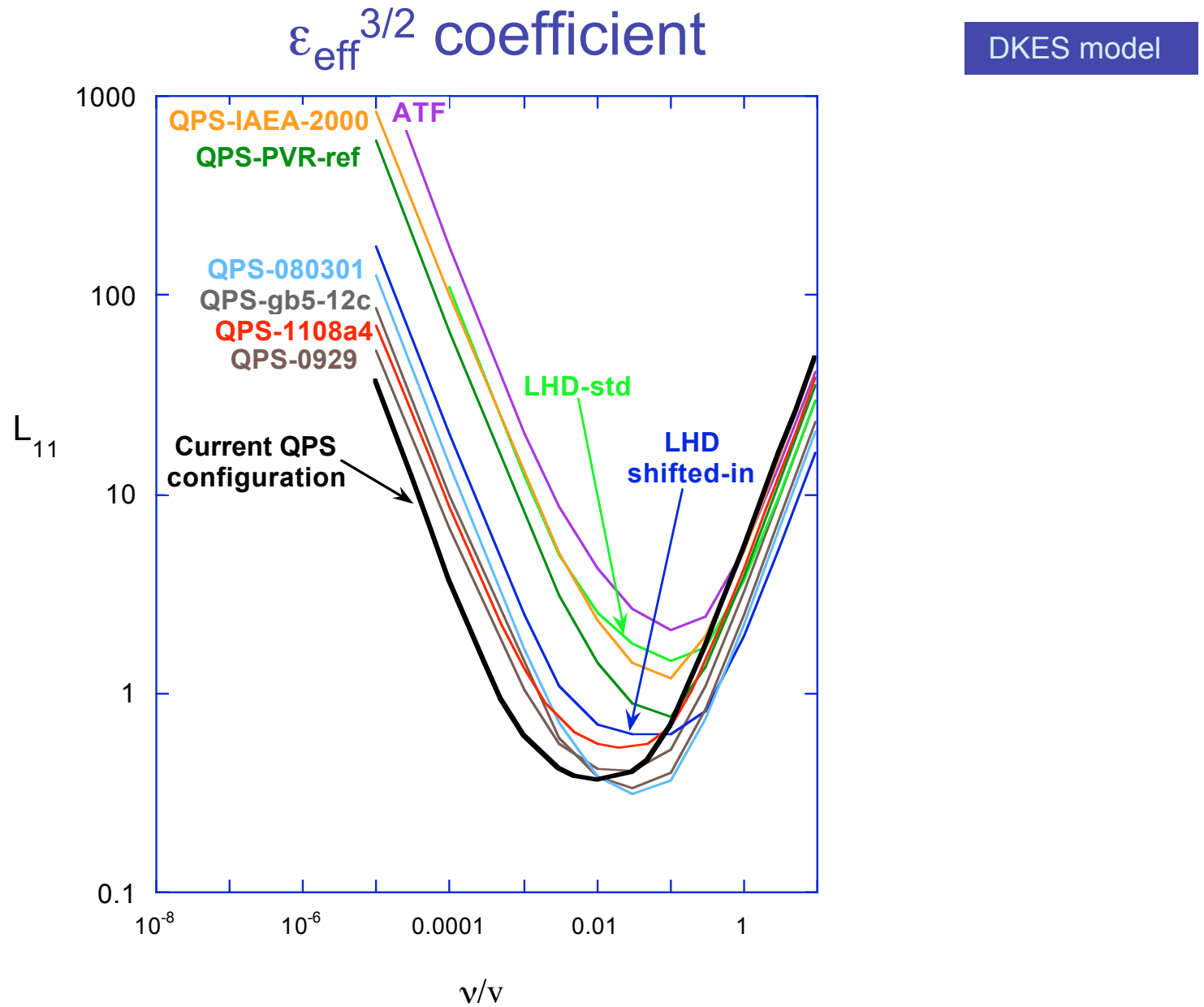


NEO code provides $\Delta_{\text{eff}}^{3/2} \sim D^{1/\beta}, \beta^{1/\beta}$. Comparison of different configurations:

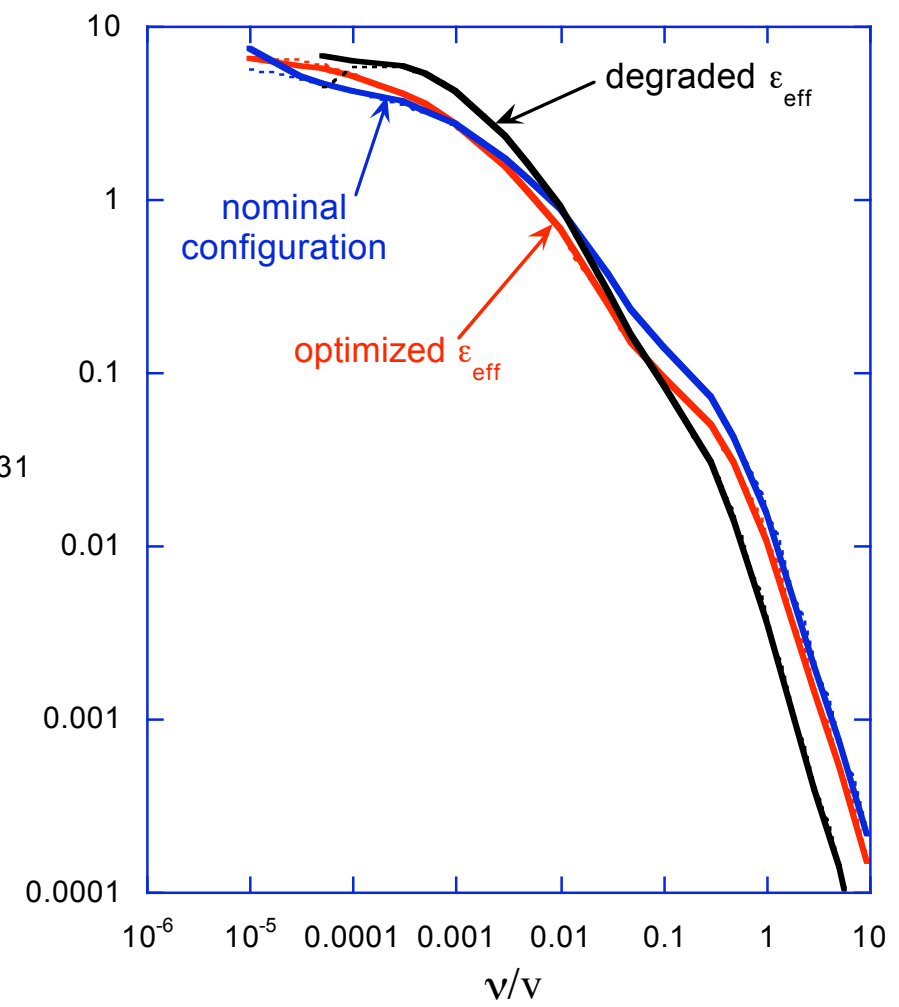
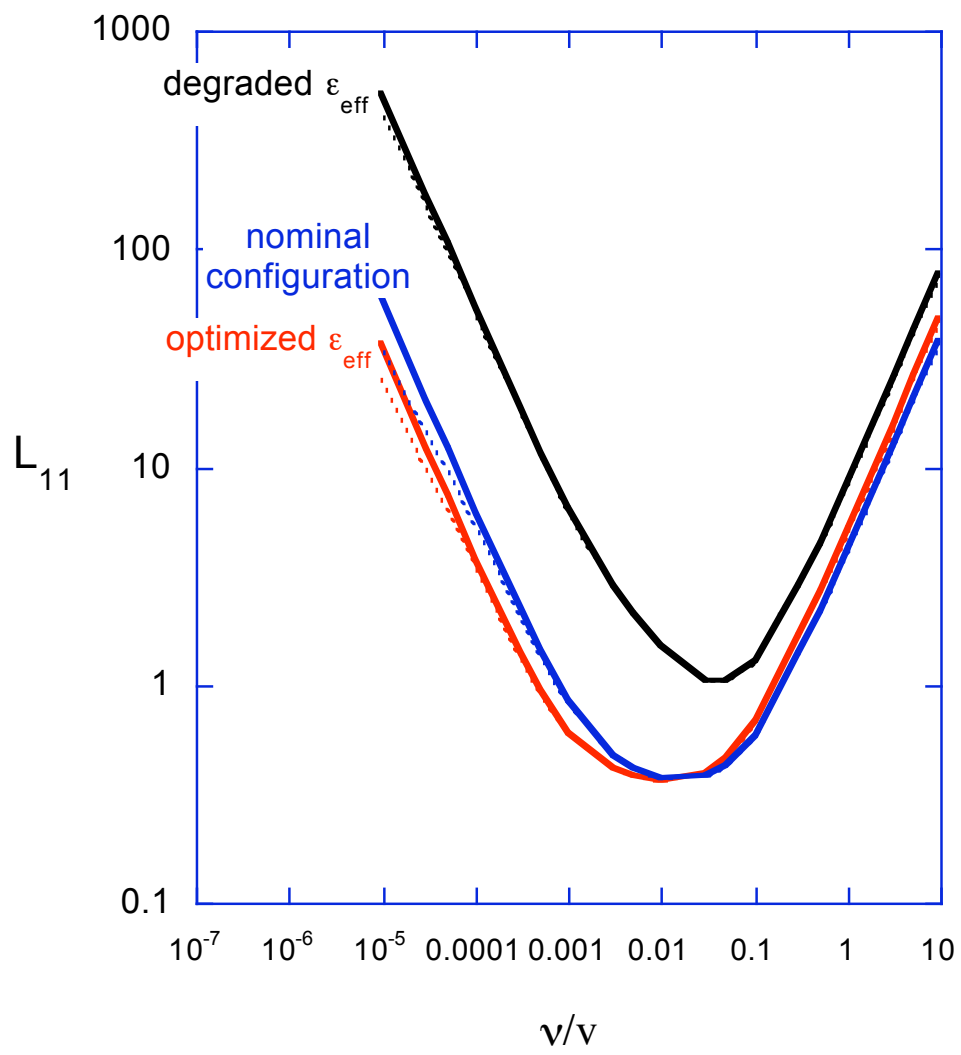
NEO Δ_{eff} code



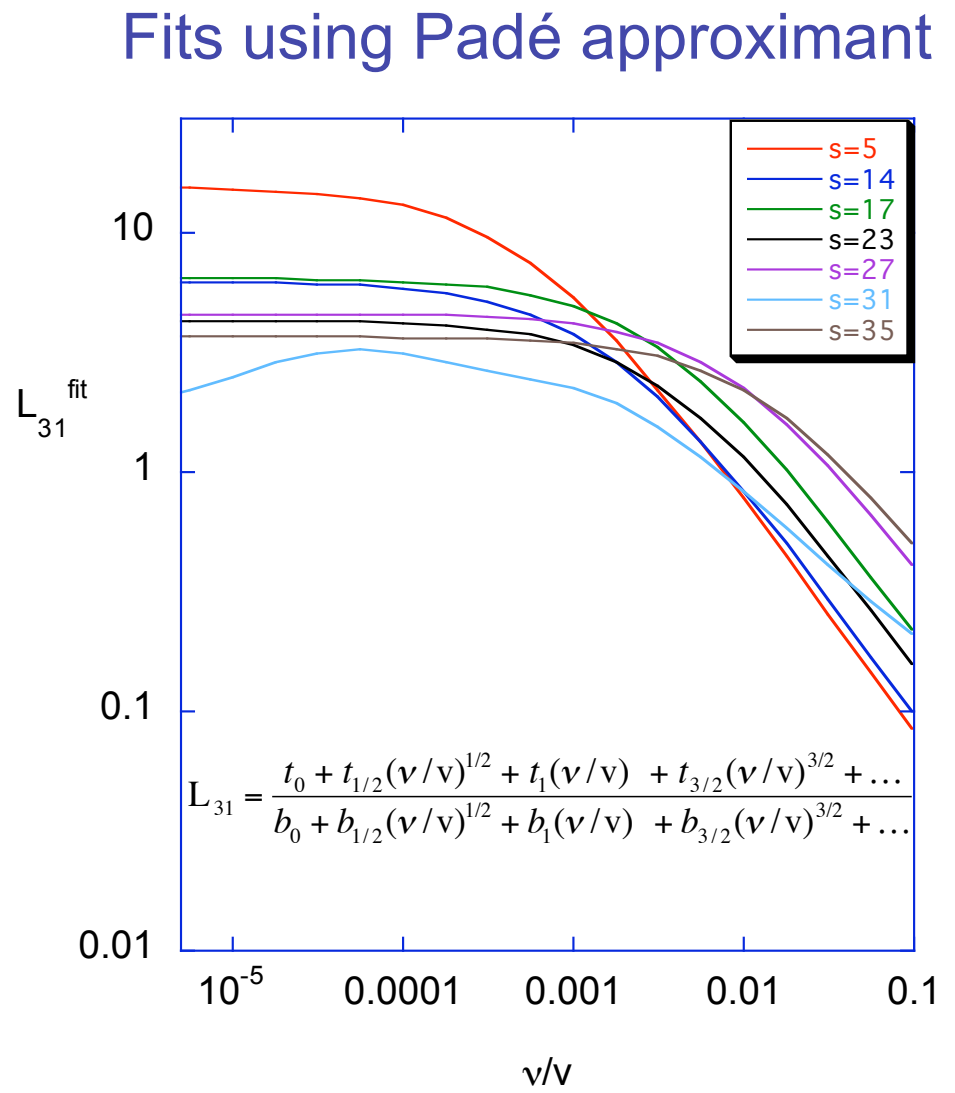
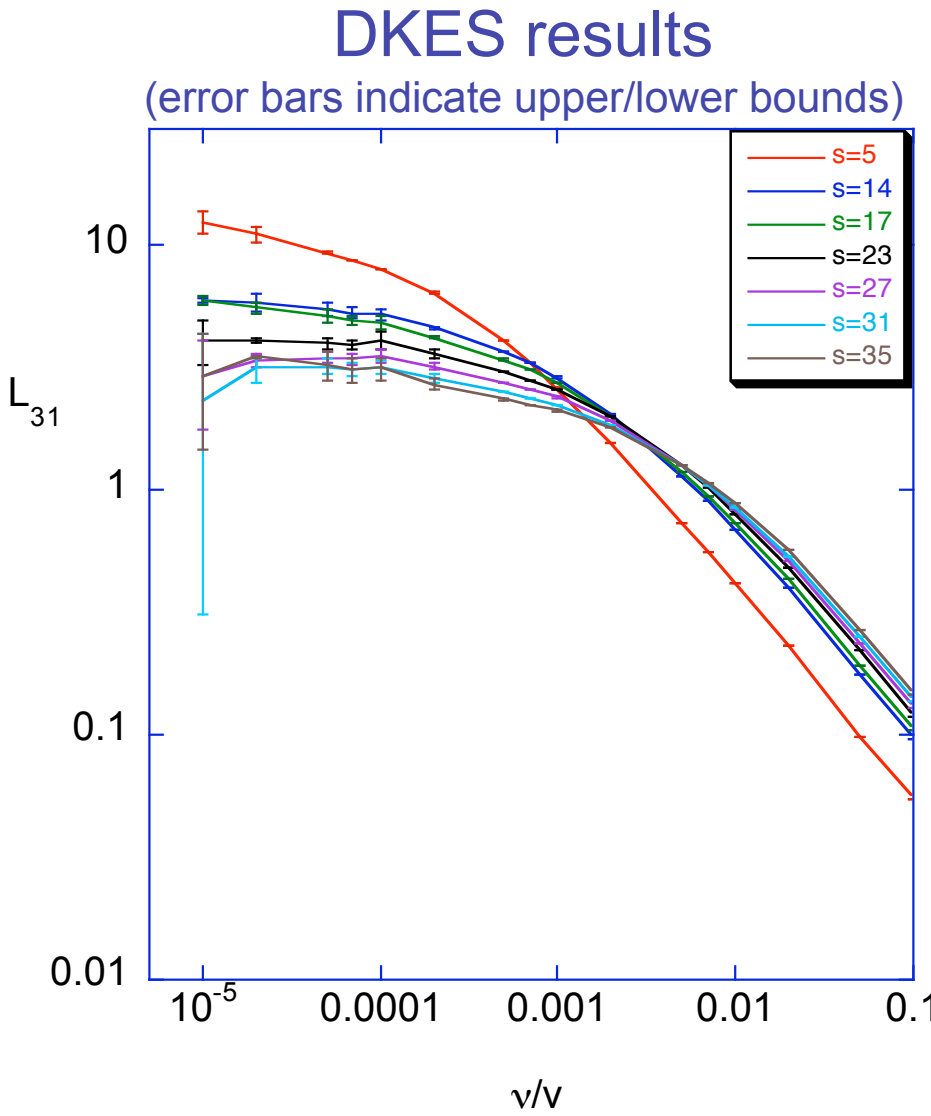
DKES L_{11} transport coefficient at $E_r/v = 0$ shows similar trends at low collisionality among QPS devices as NEO



DKES L_{11} coefficient demonstrates sensitivity of transport to coil current optimization

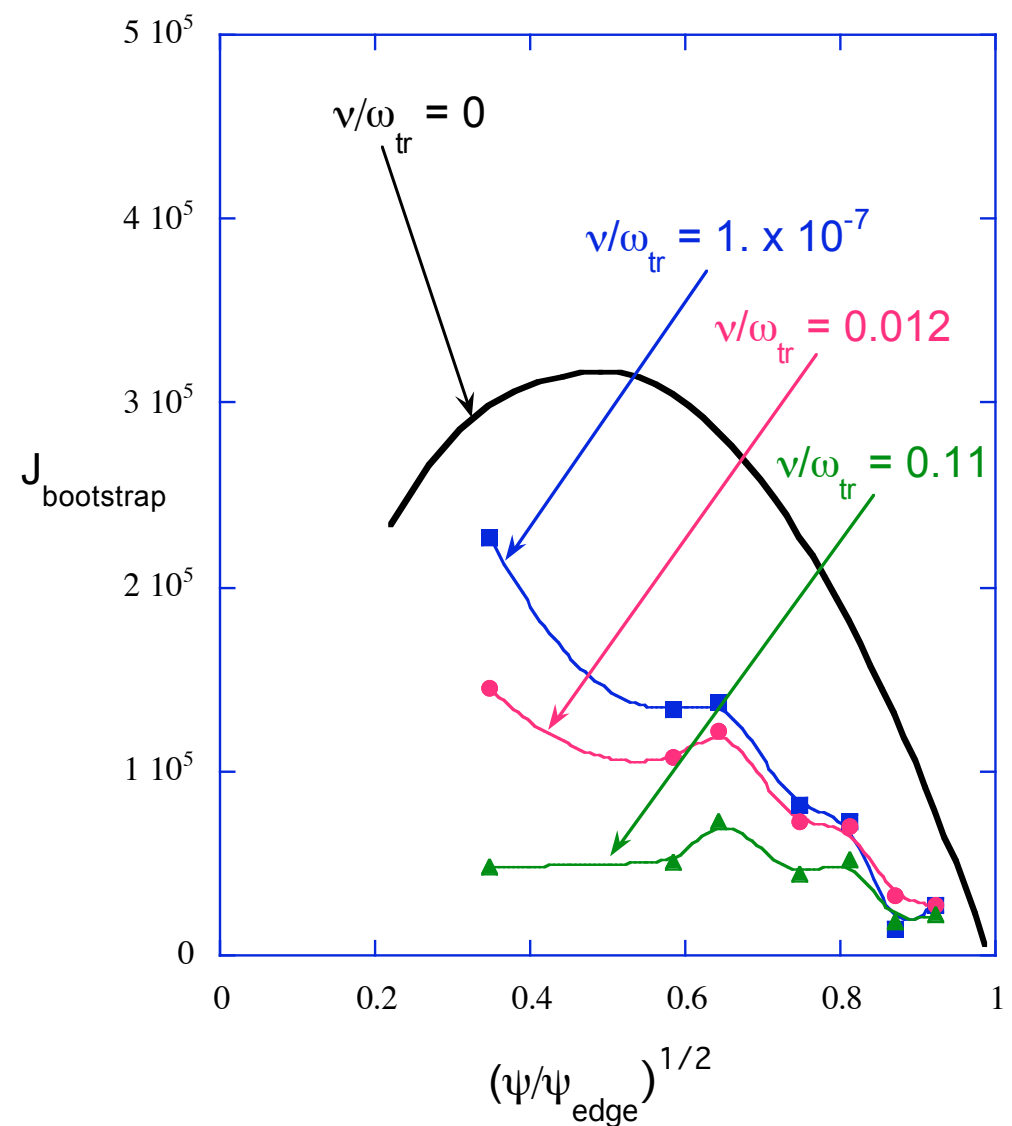


DKES L_{31} coefficient (bootstrap current for recent QPS device (411))



Comparison of DKES predicted bootstrap current profiles with collisionless limit

- Collisionless limit based on BOOTSJ code of L. Berry/J. Tolliver - includes damping to avoid singularities at rational surfaces
- Based on:
 - K.C. Shaing, B.A. Carreras, N. Dominguez, V.E. Lynch, J.S. Tolliver, "Bootstrap current control in stellarators", Phys. Fluids B1, 1663 (1989)
 - K.C. Shaing, E.C. Crume, Jr., J.S. Tolliver, S.P. Hirshman, W.I. van Rij. "Bootstrap current and parallel viscosity in the low collisionality regime in toroidal plasmas", Phys. Fluids B1, 148 (1989).
 - K.C. Shaing, S.P. Hirshman, J.S. Tolliver "Parallel viscosity-driven neoclassical fluxes in the banana regime in nonsymmetrical Toroidal plasmas", Phys. Fluids 29, 2548 (1986).

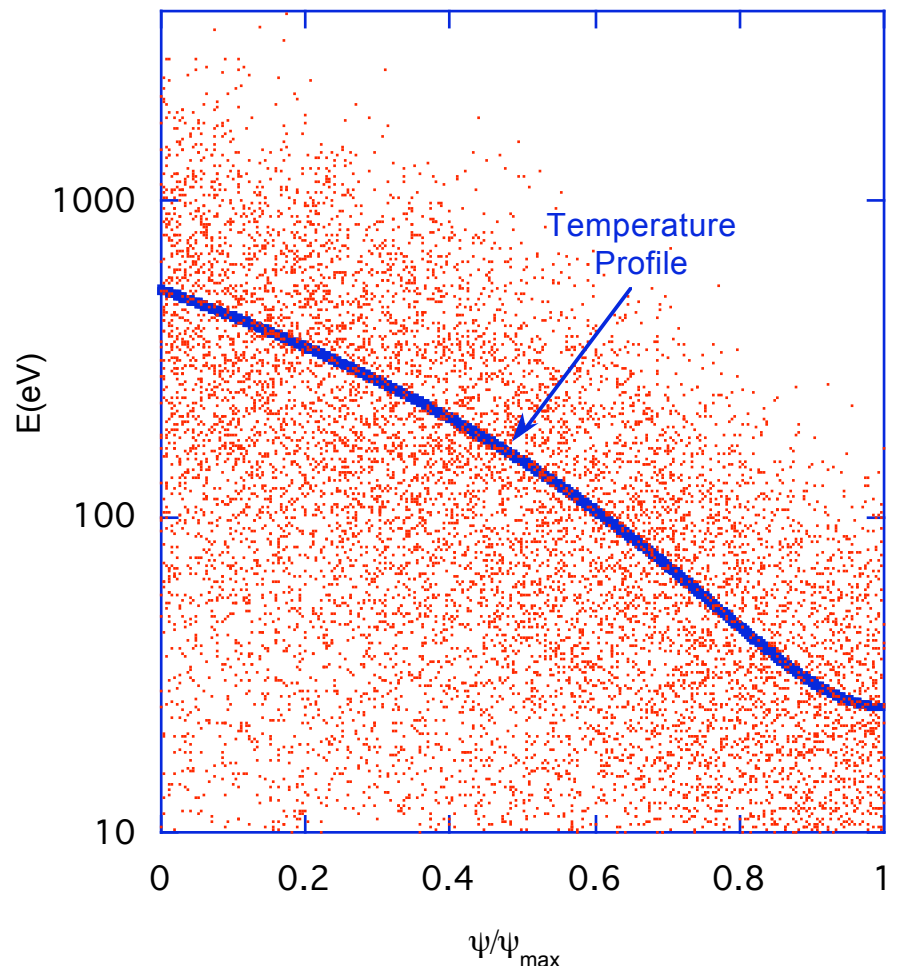


Monte Carlo procedure for estimating global energy lifetimes (DELTA5D code)

DELTA5D Monte Carlo

- start with particles distributed over cross section using PDF's consistent with assumed profiles and local Maxwellians
- follow ensemble in time, replacing particles (consistent with initial PDF's) as they leave outer surface
- Record energies of escaping particles - use to calculate \bar{E}
- Follow until approximate steady-state is achieved
- Vary potential (with fixed profile shape) to achieve global ambipolar balance of electron/ion particle loss rates

Typical initial Maxwellian particle loading for $T = 500\text{eV}$ $(1 - \frac{\theta}{\theta_{\max}})^2$



Power flows for global single species test particle simulations:

- To achieve steady state, in a reasonable simulation time, terms (1) and (2) need to be balanced:
- For $E_r = 0$
 - can include pitch angle and energy scattering if $Q_{ii} + Q_{ei}$ is weak during particle confinement time
 - or can include only pitch angle scattering
- For $E_r \neq 0$
 - rely on $Q_{ii} + Q_{ei}$ term (1) to redistribute energy loss/gain from term (2)
 - or can remove kinetic energy loss/gain (due to $e\Box\Box$) each time step

DELTA5D Monte Carlo

$$\frac{dW_{test,ion}}{dt} = \boxed{\square}(Q_{ii} + Q_{ei})d^3v \quad (+/-) \quad (1)$$

$$+ \boxed{\vec{J} \bullet \vec{E}} d^3v \quad (+/-) \quad (2)$$

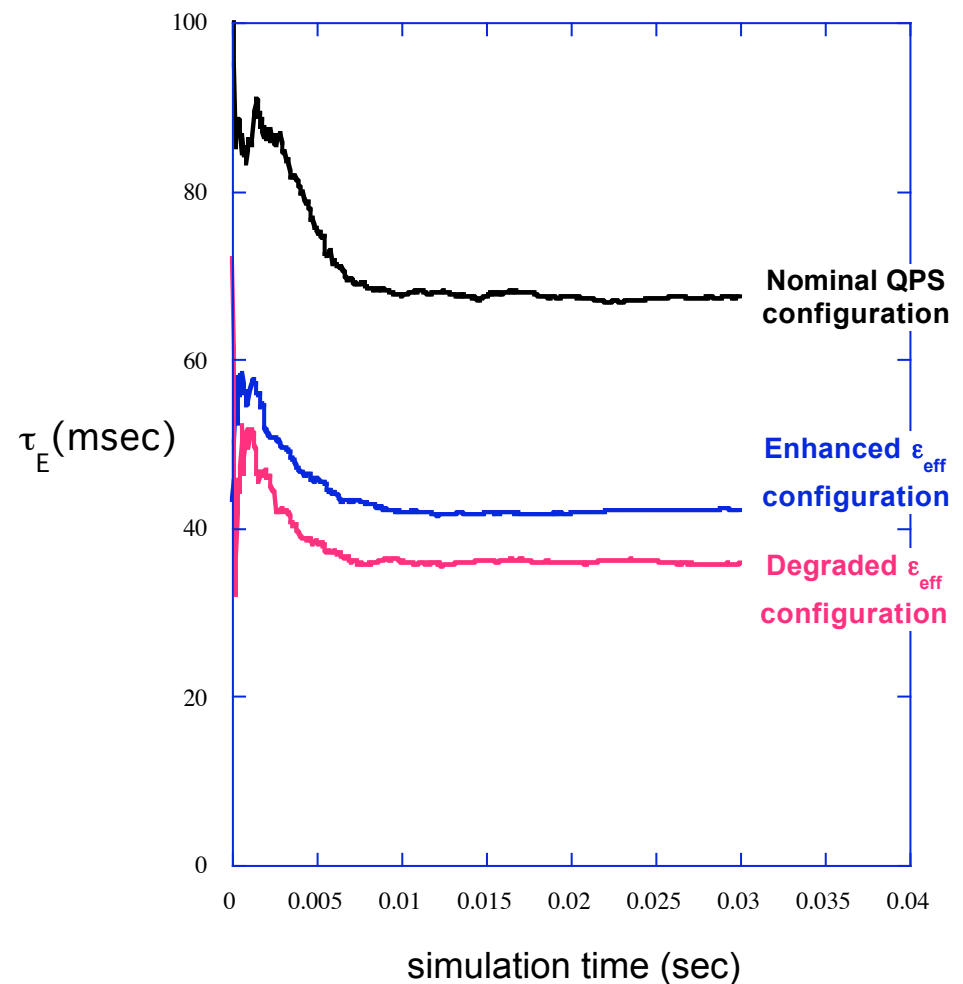
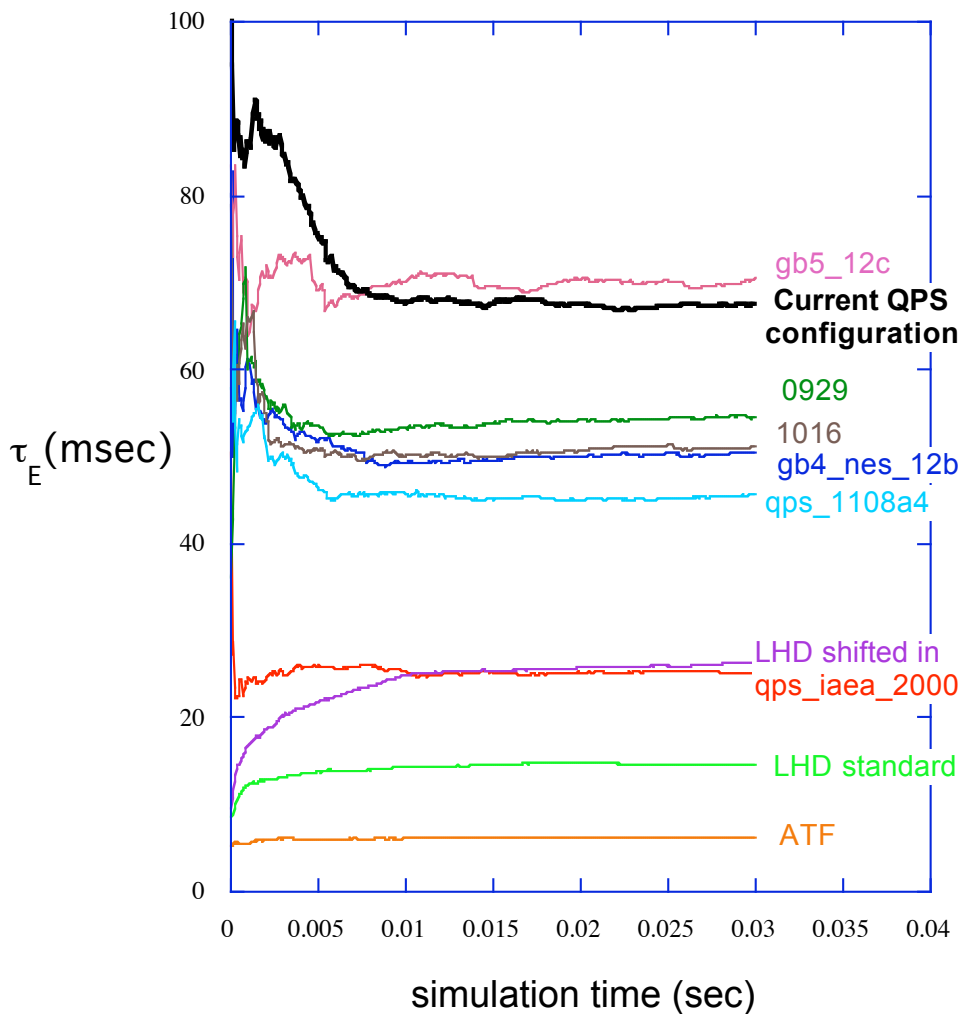
$$+ \boxed{\frac{dW_{surface\Box loss}}{dt} dS} \quad (-) \quad (3)$$

$$+ \boxed{\frac{dW_{surface\Box loss}}{dt} dS} \quad (+/-) \quad (4)$$

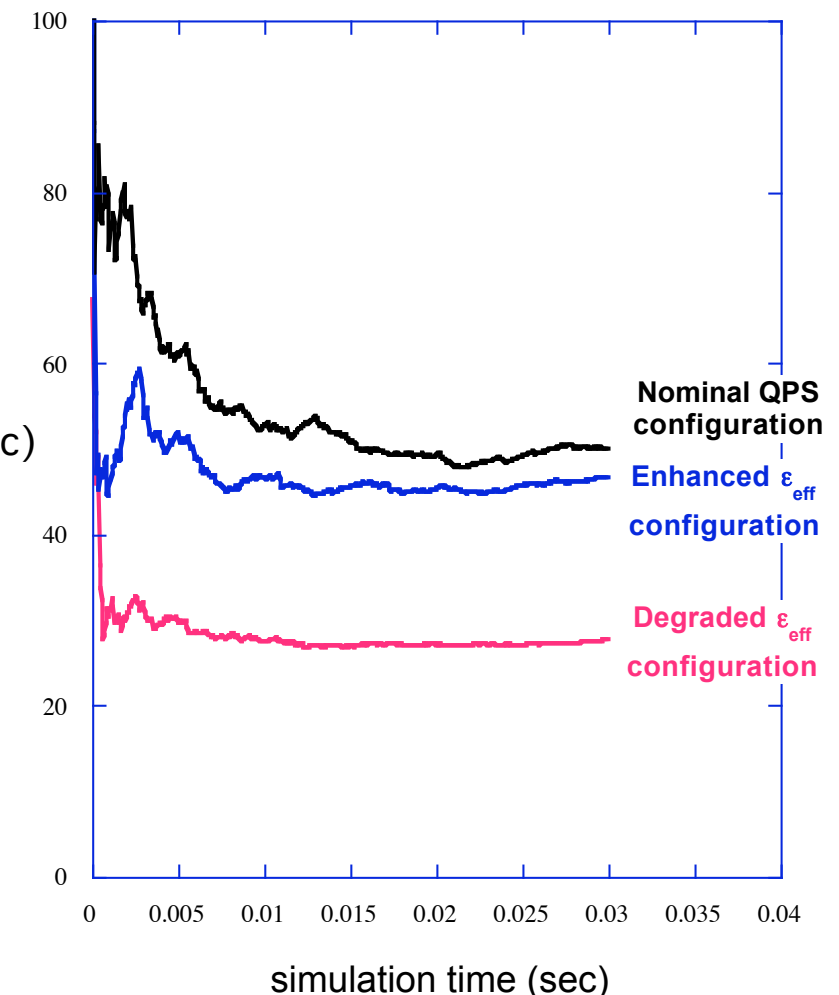
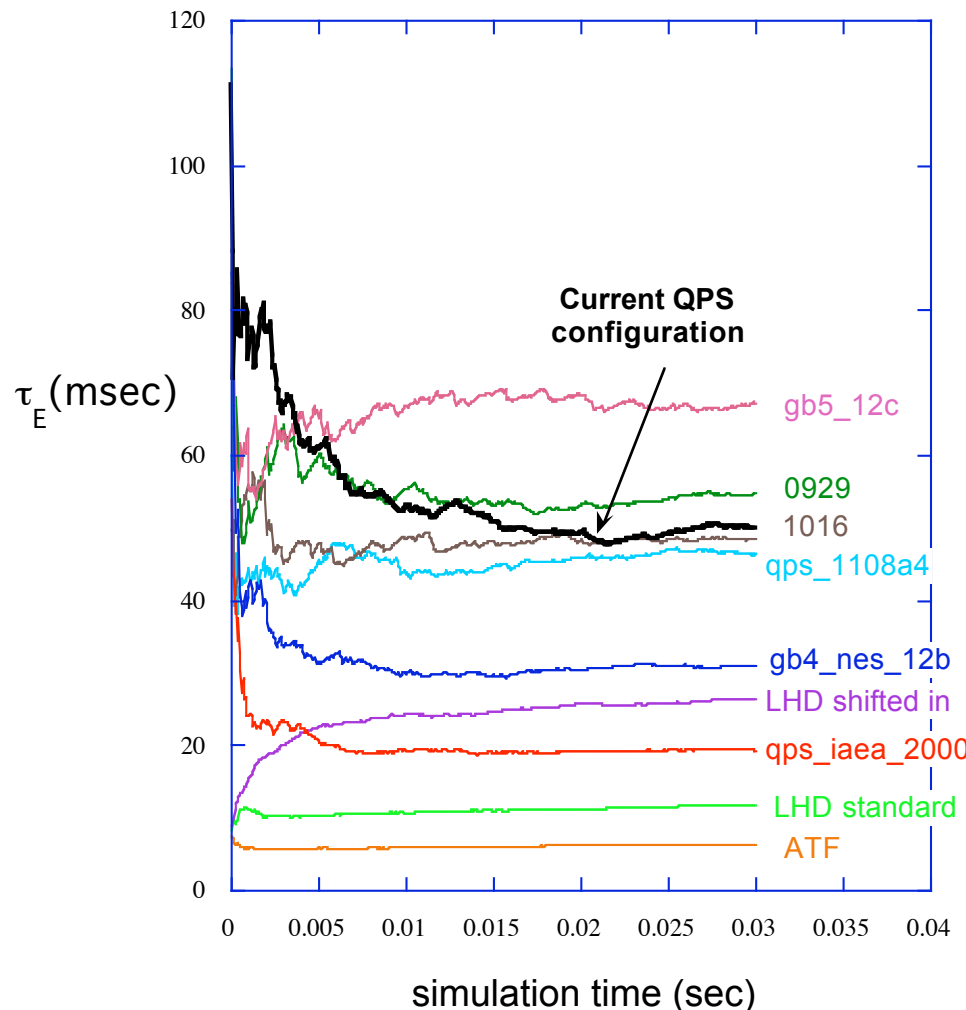
$$+ \boxed{N_{replacement} [T(\Box) + e\Box]} d^3v$$

$\frac{dW_{test,electron}}{dt} =$ Similar equations

Monte Carlo studies of global ion confinement times for ICH parameters between devices (all at same R_0) and for different coil currents



Monte Carlo studies of global ion confinement times for ECH parameters between devices (all at same R_0) and in QPS for different coil currents

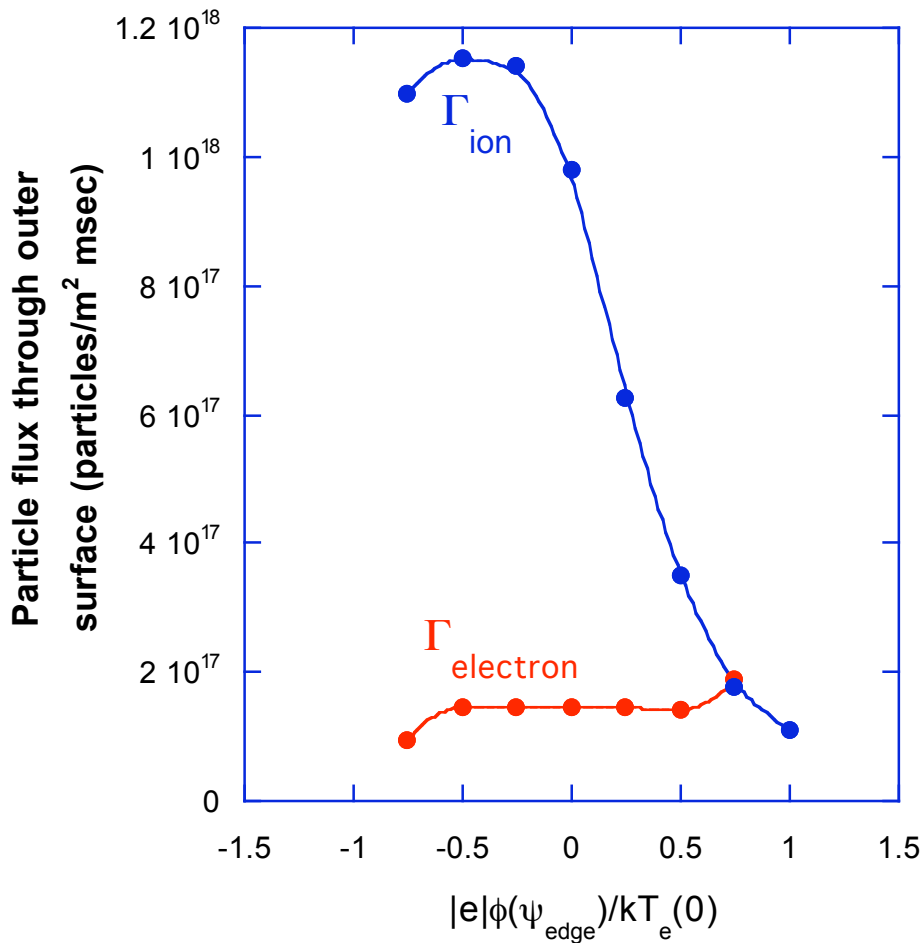


Monte Carlo (DELTA5D)

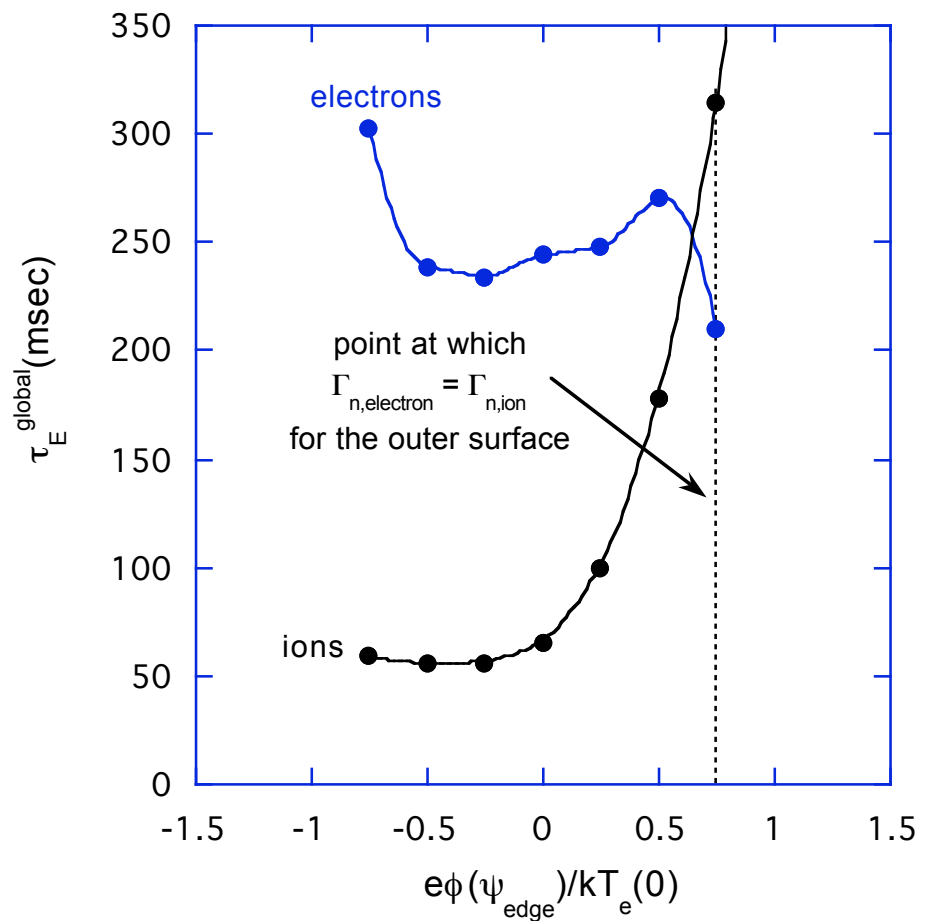
Monte Carlo lifetimes for ICH heated gb4 configuration

$[n(0) = 8.3 \times 10^{19} \text{ m}^{-3}$, $T_e(0) = 500 \text{ eV}$, $T_i(0) = 500 \text{ eV}$, flat density profile, parabolic**2 temperature profile]

Global ambipolarity condition
[i.e., with $\mathbb{B}(r)$ profile fixed]

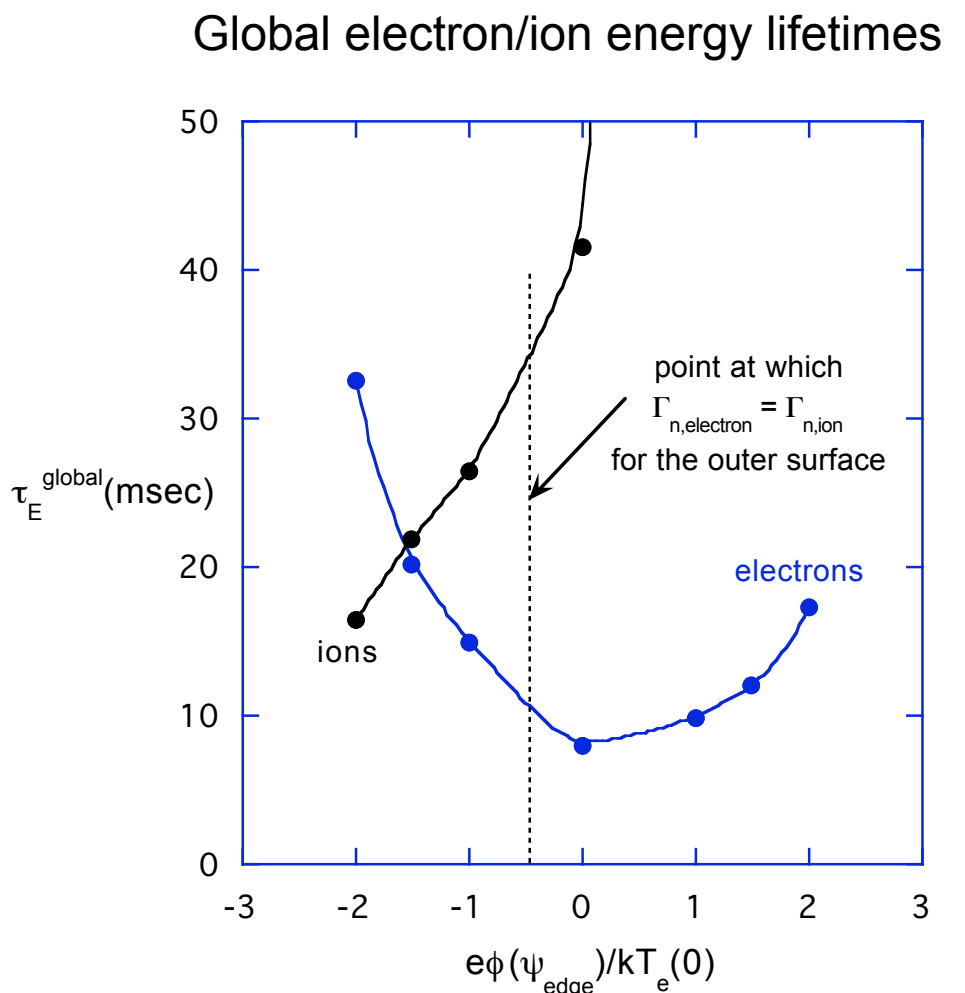
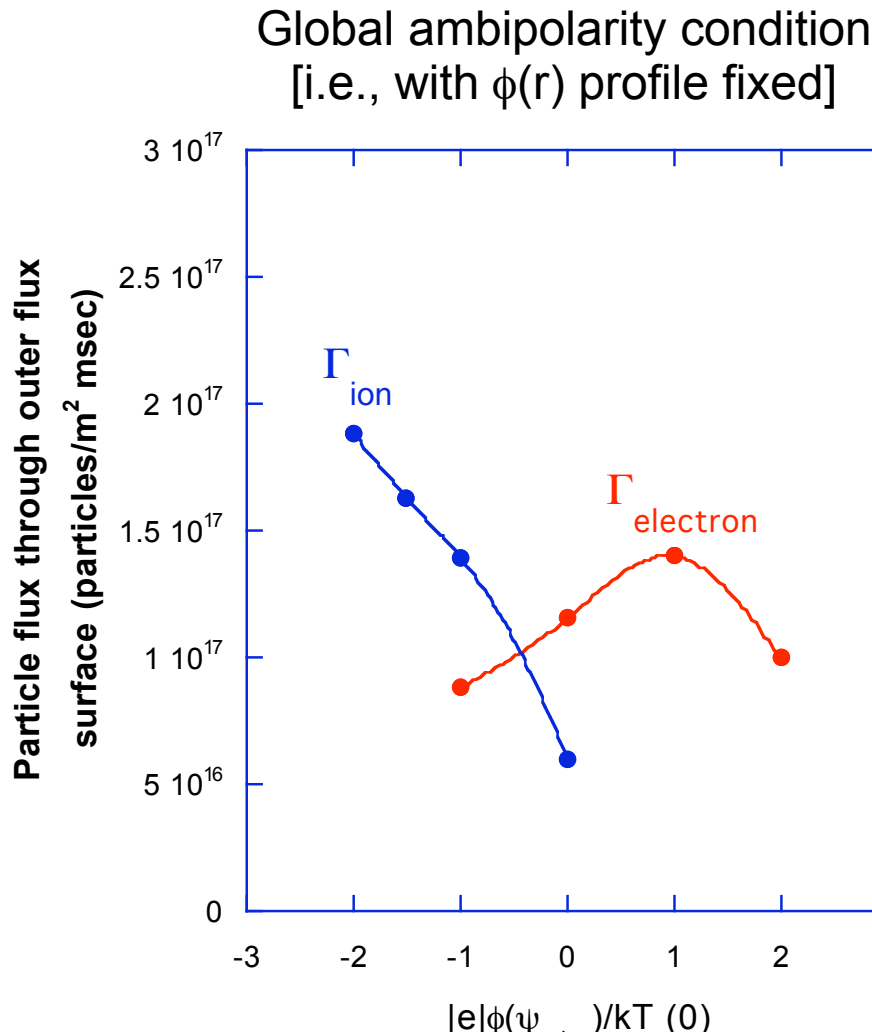


Global electron/ion energy lifetimes

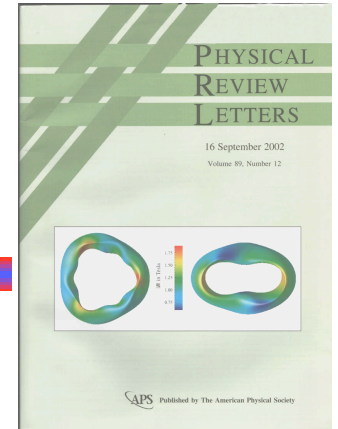


Monte Carlo lifetimes for ECH heated gb4 configuration

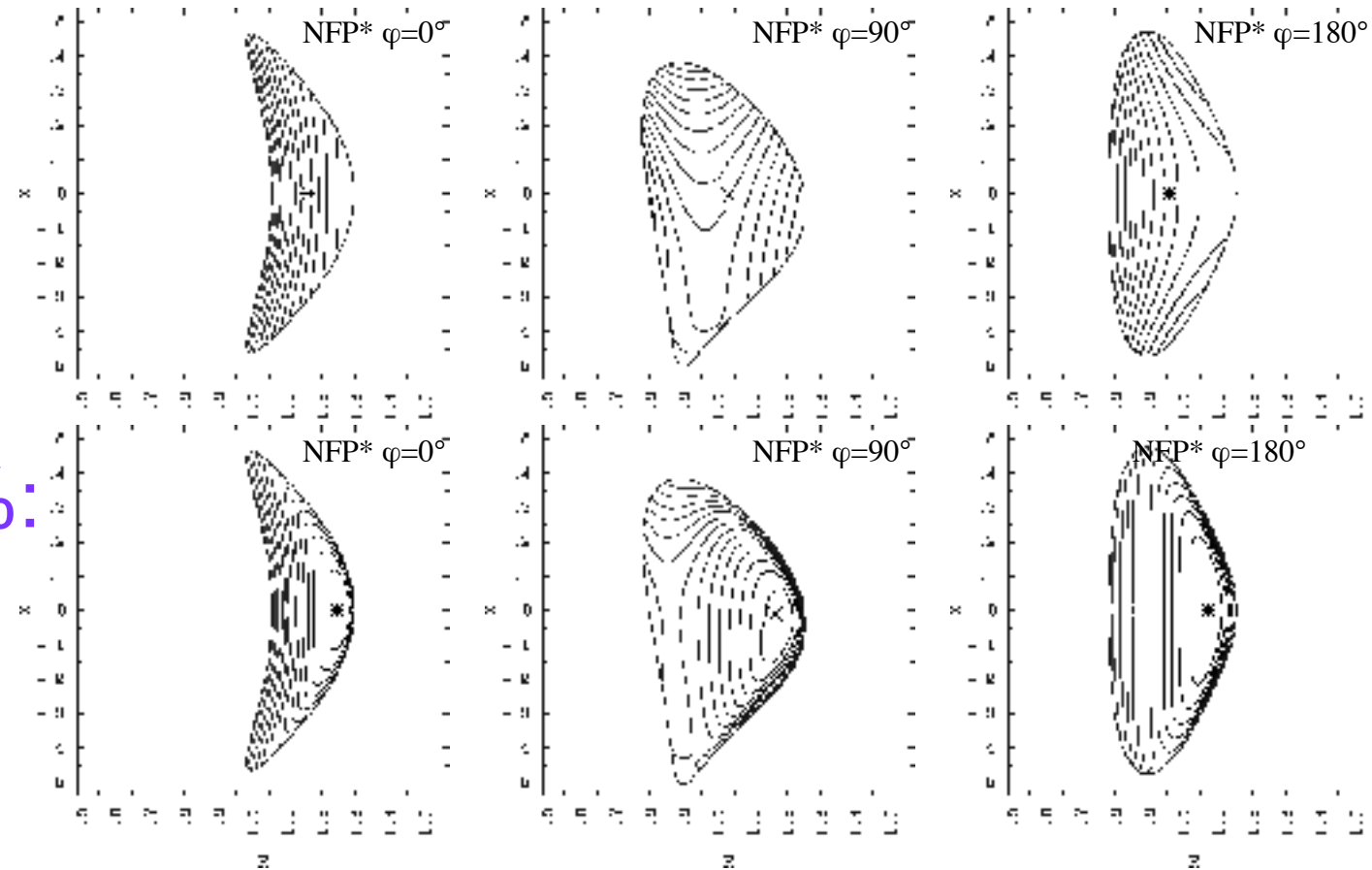
$[n(0) = 1.8 \times 10^{19} \text{ m}^{-3}$, $T_e(0) = 1400 \text{ eV}$, $T_i(0) = 150 \text{ eV}$, flat density profile, parabolic **2 temperature profile]



High \square configuration: $|B|$ contours and flux surfaces become aligned



$\square=0\%:$

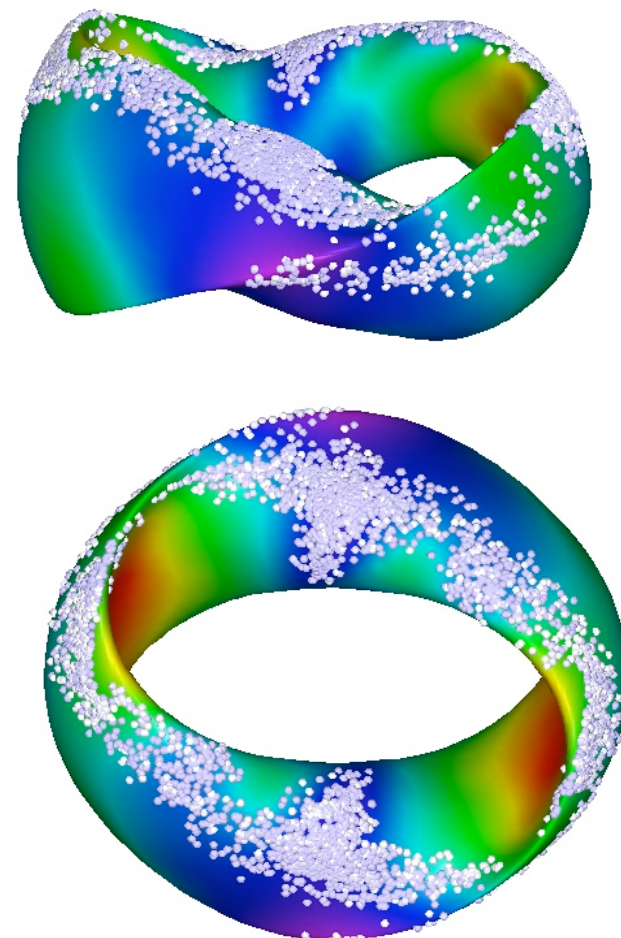
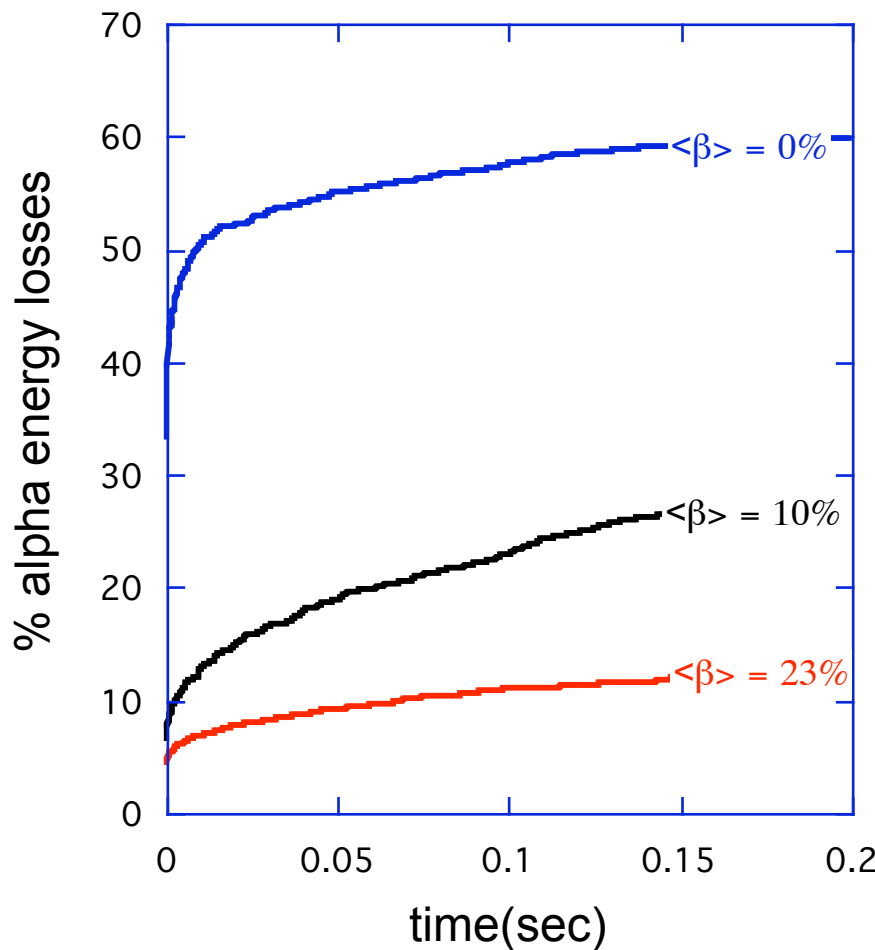


$\square=23\%:$

\square -particle slowing-down simulations show these devices indicate very good confinement with increasing \square .

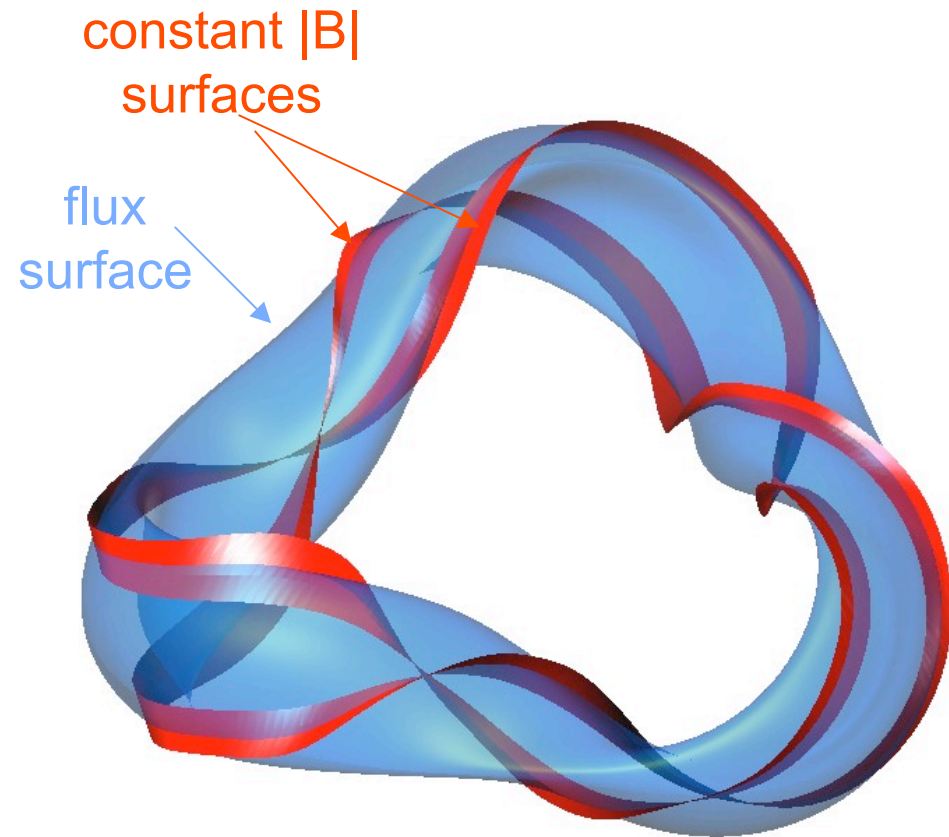
Transport analysis

The configuration was scaled to $\langle B \rangle = 5T$ and $R_0 = 10m$ for alpha confinement studies



ICRF heating in stellarators depends on wave propagation, geometry of the resonant regions and the orbit confinement of the resonant ions

- Confinement of ICRF heated ions is examined by following a collection of orbits
- Intersections of $|B|$ contours with flux surfaces are determined for inner half of the plasma volume
- Ions are started out at $B = B_{\text{res}}$ with $v_{||0}/v = 0$ (equivalent to $\dot{\theta}/\dot{\phi} = B_{\text{res}}$)
- Ions leaving the outer surface are removed from the population



Local Monte-Carlo equivalent quasilinear ICRF operator (developed by J. Carlsson)

$$E^+ = E^0 + \square^E + \square\sqrt{\square^{EE}}$$

$$\square^+ = \square^0 + \square^I + \square\sqrt{\square^{II}}$$

\square = a zero mean, unit variance random number (i.e., $\langle \square^0 \rangle = 0$ and $\langle \square^I \rangle = 1$)

$$\square^{EE} = 2m^2 v_{||}^2 \square v_0$$

$$\square^{II} = 2 \frac{k_{||} v_{||}}{v} \square \frac{v_{||}^2}{v^2} \frac{v_{||}^3 \square v_0}{v^2}$$

$$\square^E = 2 \frac{1}{\square} \frac{k_{||} v_{||}}{v} \square m v_{||} \square v_0$$

$$\square^I = \frac{1}{2} \frac{1}{\square} \frac{k_{||} v_{||}}{v} \square \frac{v_{||}^2}{v^2} \frac{k_{||}}{\square} \square \frac{v_{||}}{v^2} + \frac{v_{||}}{v^2} \frac{v_{||}^2}{v^2} \frac{v_{||} \square v_0}{v}$$

where

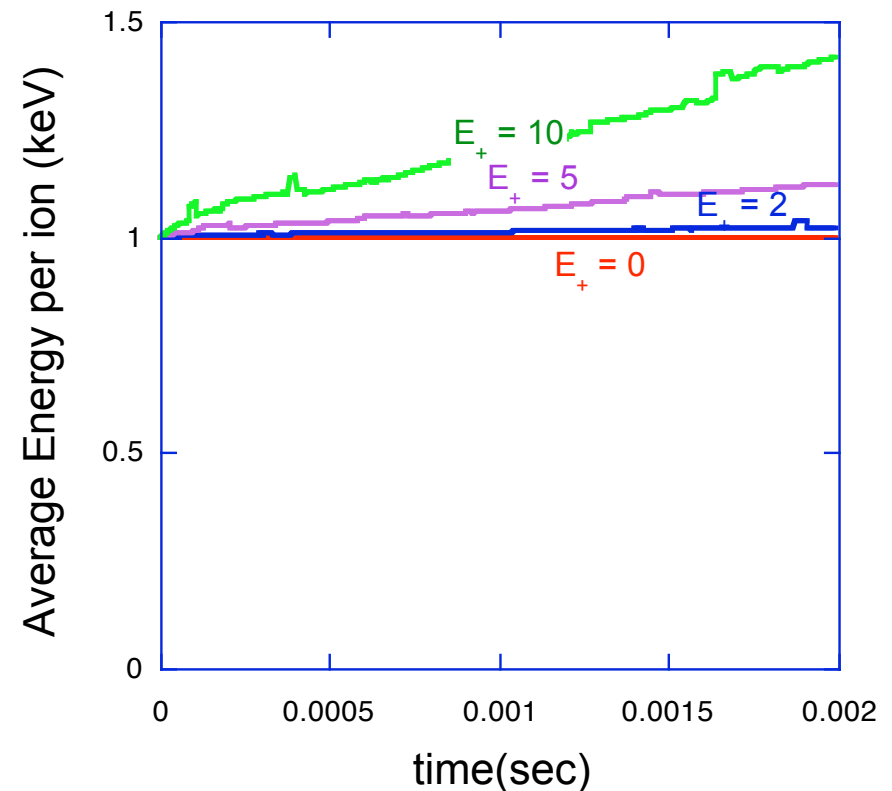
$$\square v_0 = \frac{1}{v_{||}} \frac{eZ}{2m} |E_+ J_{n||}(k_{||} \square) + E_- J_{n+1||}(k_{||} \square)|^2 \frac{2 \square}{n \dot{\square}}$$

as $\dot{\square} \rightarrow 0$

$$\frac{2 \square}{n \dot{\square}} \rightarrow 2 \square^2 \left| \frac{2}{n \dot{\square}} \right|^{2/3} \square \text{Ai}^2 \left| \frac{n^2 \dot{\square}^2}{4} \left| \frac{2}{n \dot{\square}} \right| \right|^{4/3}$$

Monte Carlo simulation of ICRF heating in stellarators

- Quasi-linear ICRF diffusion operator (follows particles as they are kicked up in energy)
 - Intersections of $|B|$ contours with flux surfaces determined
 - Ions are started out at $B = B_{\text{res}}$ with $v_{\parallel 0}/v = 0$ (equivalent to $\bar{v}/v = \bar{B}/B_{\text{res}}$)
- Simple RF wave-field model:
 $k_{\parallel} = n/2\pi R_0$, $n = 1$, $k_{\perp} = 0$
 $E_+ = E_+^0 \exp[-(r - 0.3)^2]$, $E_- = 0$
- Eventual goal is to incorporate particle simulation model with ORNL RF Full Wave codes



□f Bootstrap Current Calculation

[based on method of A. Boozer and M. Sasinowski, Phys. Plasmas **2** (1995) 610]

Substituting $f = f_M e^{\square}$ into $\frac{df}{dt} = C(f)$ gives:

$$\frac{d\square}{dt} \square C_l(f) = \square \frac{1}{f_M} \frac{\partial f_M}{\partial \square} \frac{\partial \square}{\partial t}$$

where $C_l = \text{linearized collision operator} = \frac{C(f)}{f}$

Now, define $\square = \square \frac{\square}{\partial \ln f_M / \partial \square} = \text{particle deviation from initial } \square \text{ surface}$

Expand f , assuming \square is small: $f = f_M \exp \left(\frac{\partial \ln f_M}{\partial \square} \right) \square f_M \square \square \frac{\partial f_M}{\partial \square}$

[This allows one to take into explicitly account the cancellation
of bootstrap current which occurs for f_M]

The plasma current is then given by:

$$j_{\parallel,mn} = q \int v_{\parallel} f e^{\beta_2 \ln(n/m)} d^3 v d^3 x$$

Which, using the above expansion for f , can be written as:

$$j_{\parallel,mn} = \frac{q \int v_{\parallel} \frac{\partial f_m}{\partial \beta} 2 \int v^2 dv d^3 x}{\int d^3 x J}$$

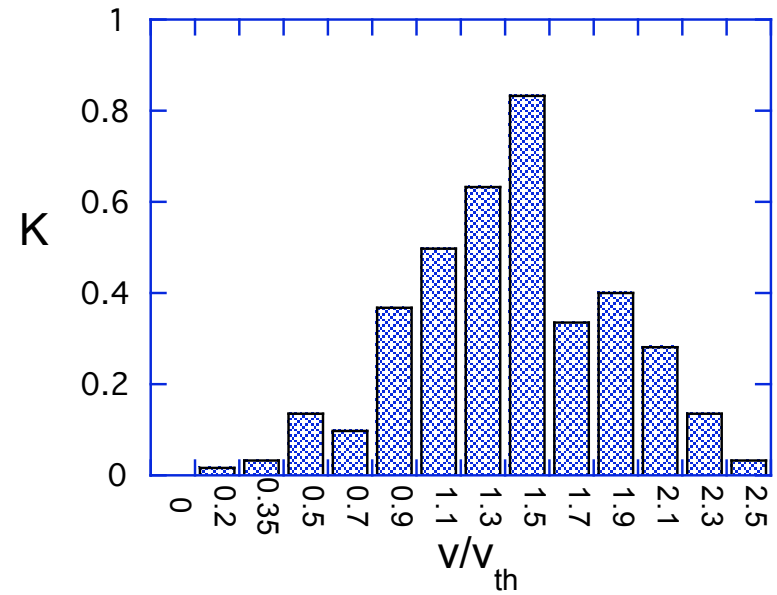
$$\text{where } J = \mu_0 (G + B) / B^2$$

Specializing to the bootstrap current ($m = 0, n = 0$), the above integral can be reduced to a sum over particles, followed by an integration over velocity:

$$K(\square, v, t) = \frac{\prod_{i=1}^N v_{||,i} \frac{\square_i}{J_i}}{2 \prod_{i=1}^N J_i}$$

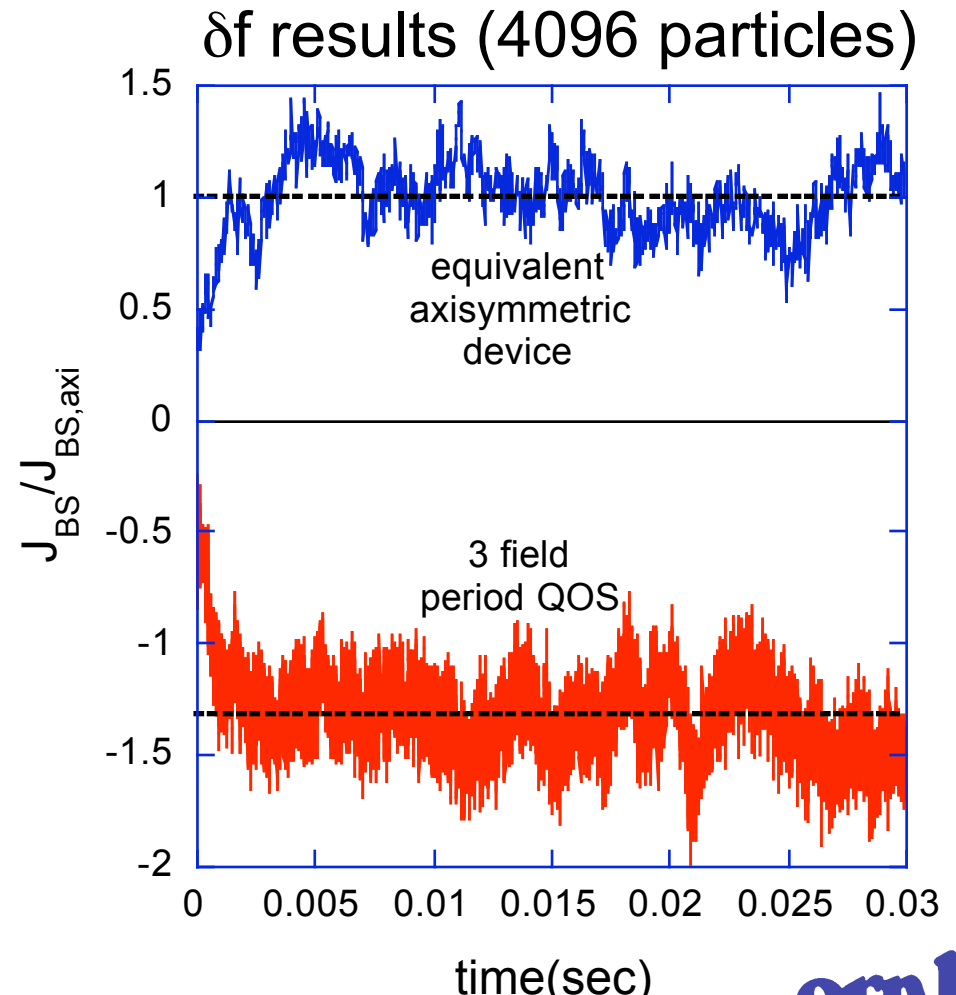
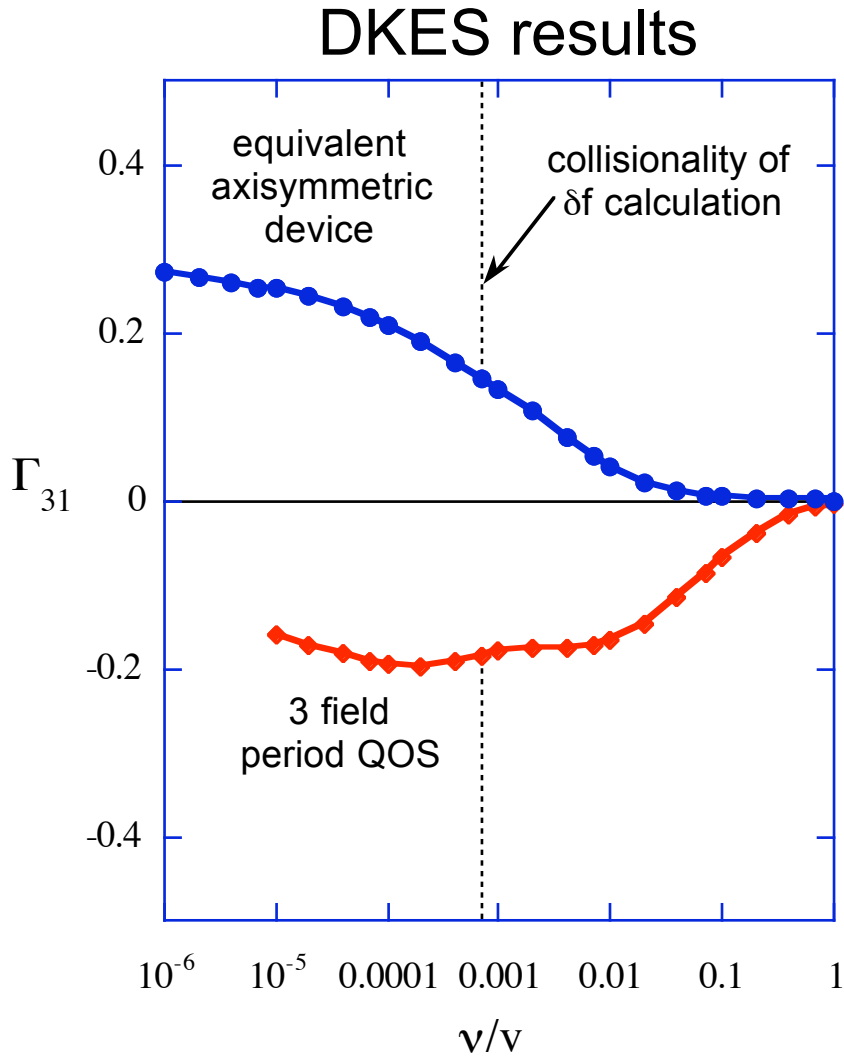
$K(\square, v, t)$ is then sorted into velocity bins, all the processors communicate these results and a sum over processors is made. Finally, the bootstrap current is obtained by integrating over these bins:

$$j_{\text{bootstrap}} = \int 4 \pi \square v^2 dv K(\square, v, t) \frac{\partial f_M}{\partial \square}$$

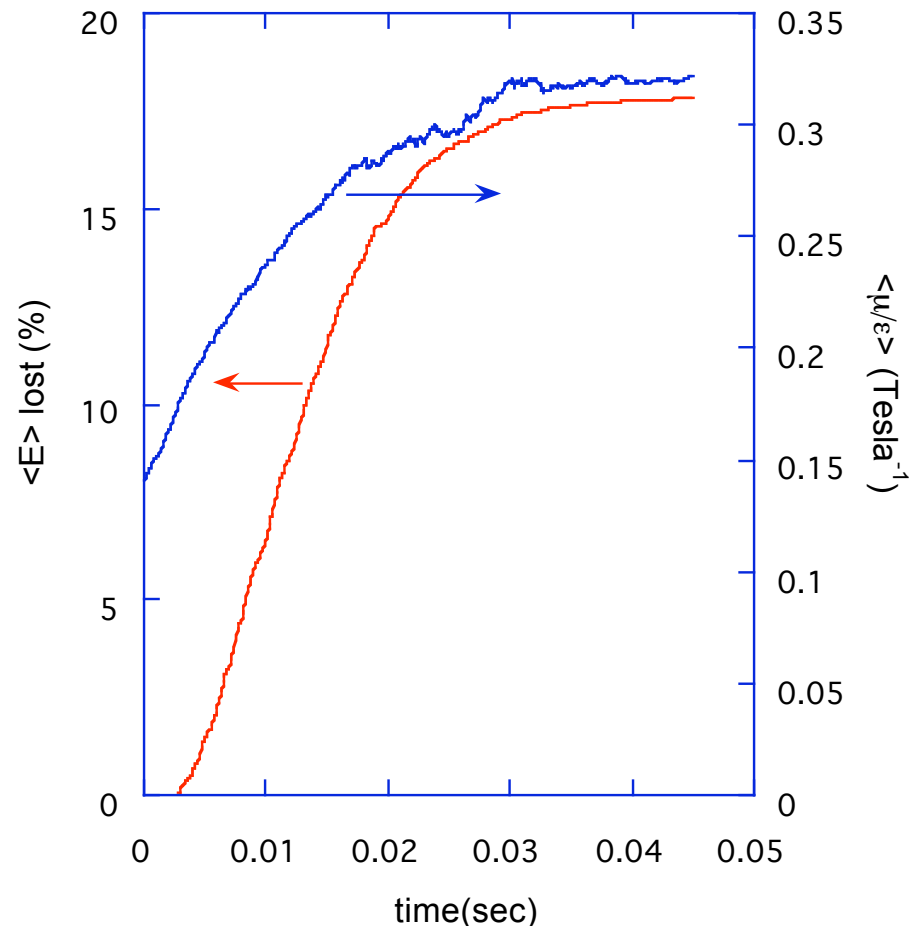
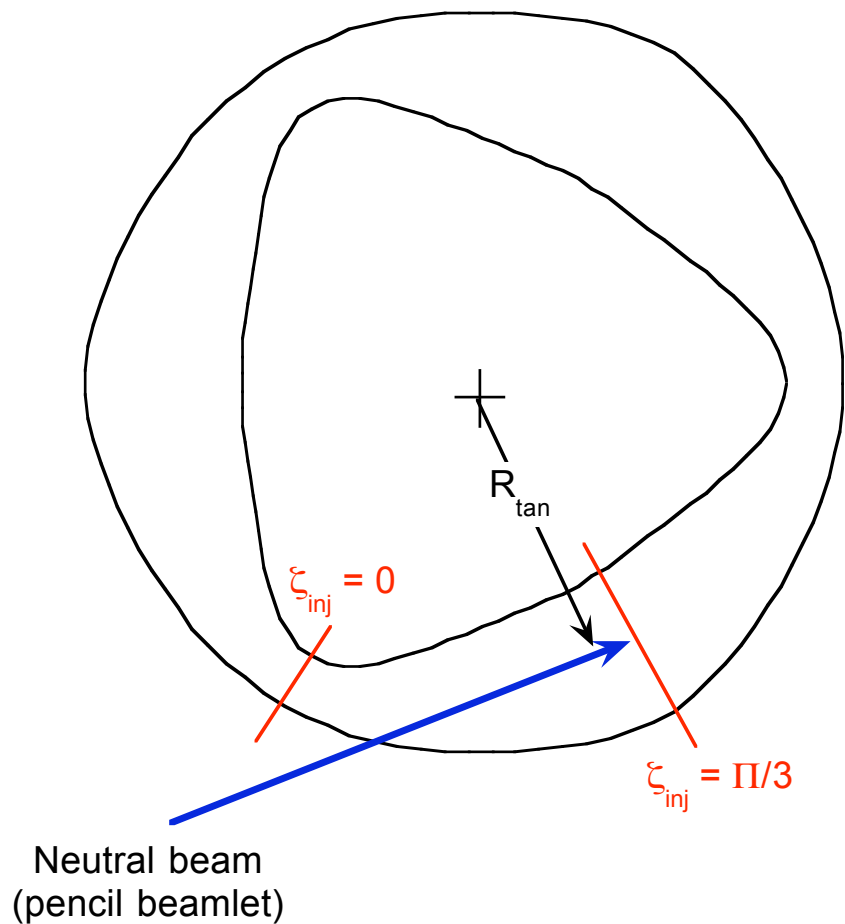


Bootstrap current levels for a QO device and its axisymmetric equivalent show agreement between DKES and the f particle code:

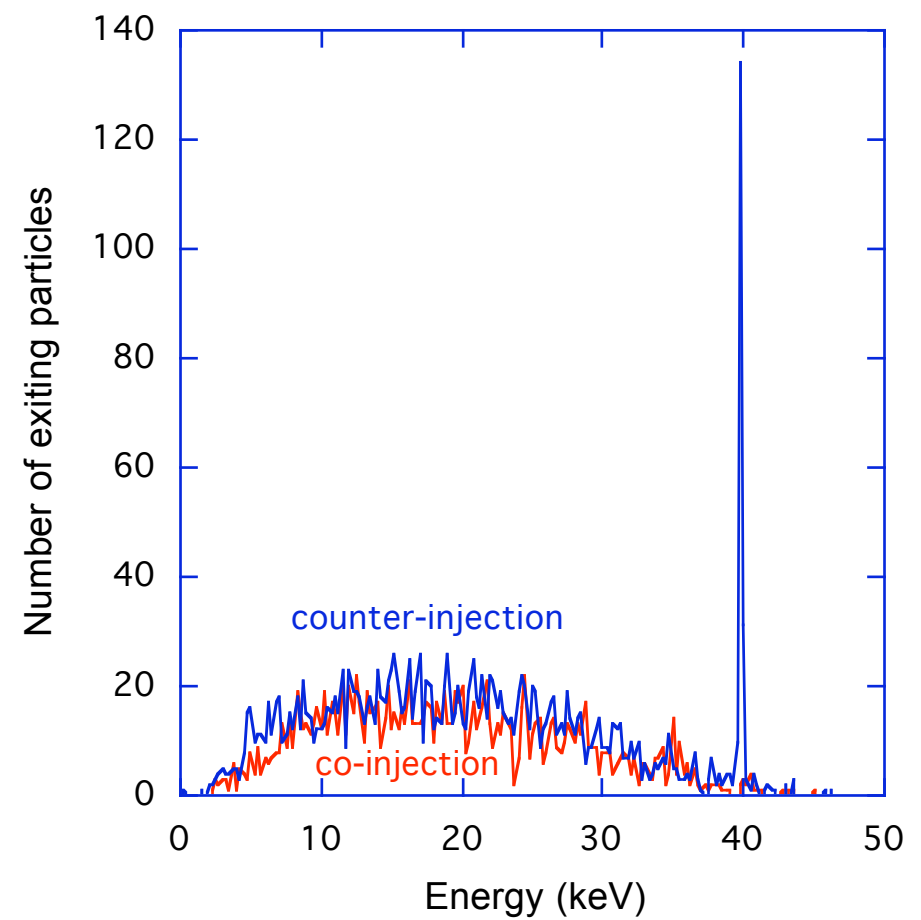
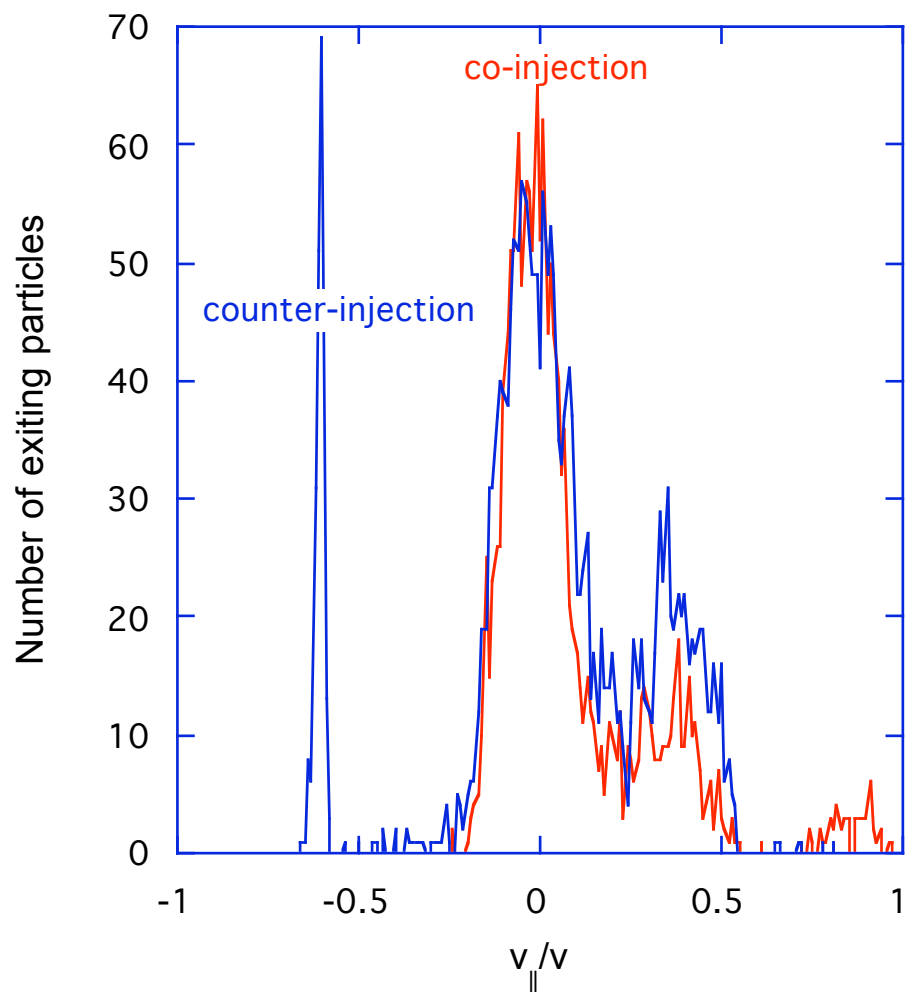
$(J_{BS}^{\text{non-axi}}/J_{BS}^{\text{axi}} = -1.309 \text{ from DKES and } = -1.32 \text{ from } \text{f})$



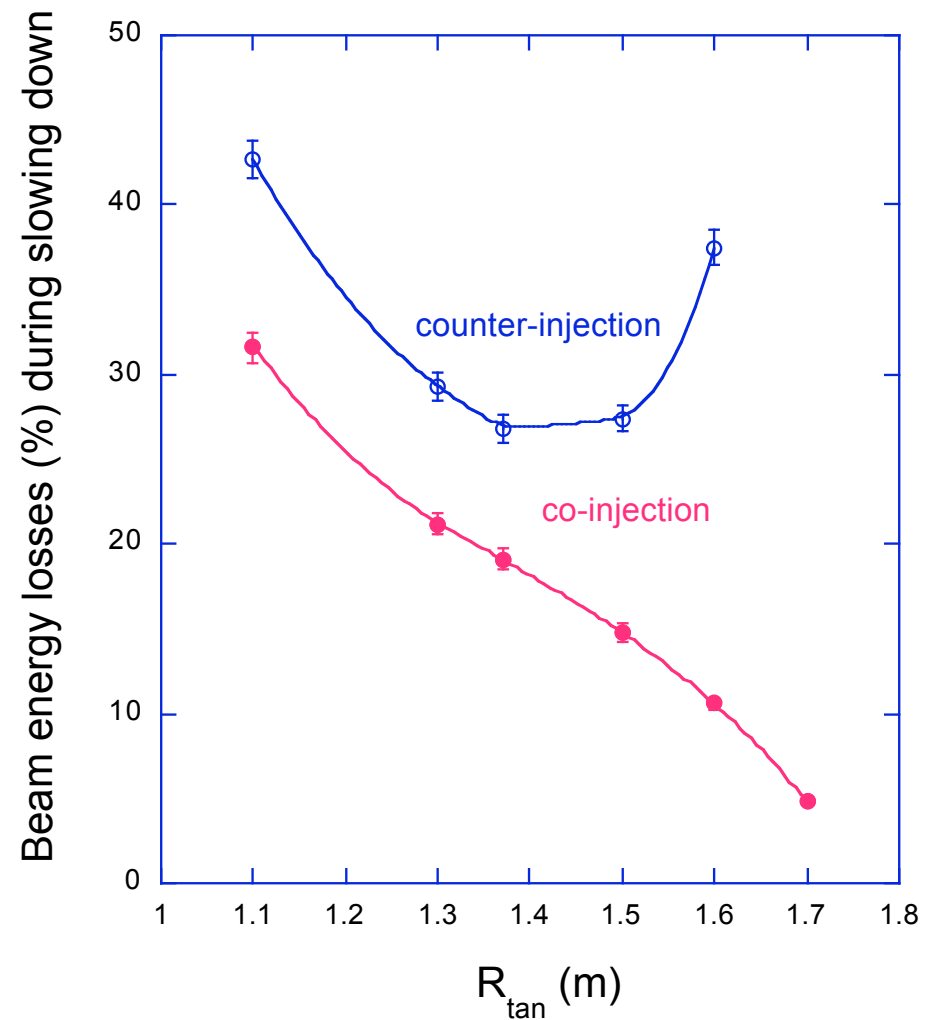
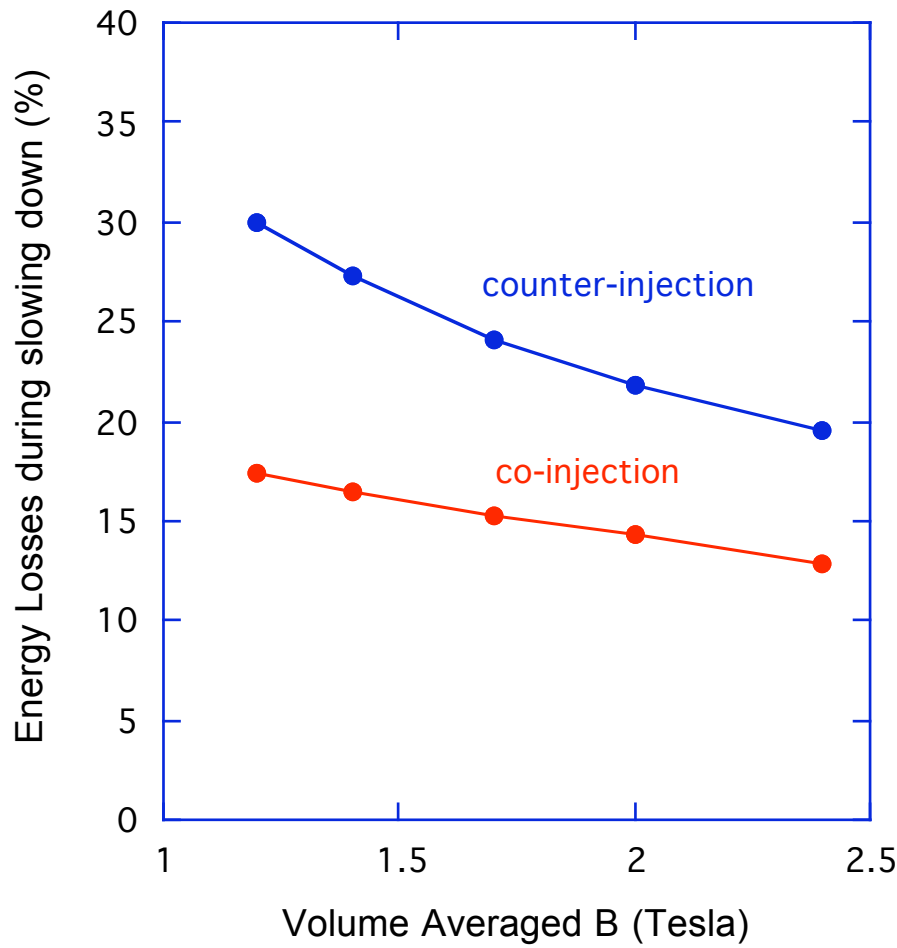
Neutral beam heating efficiency calculations: NCSX



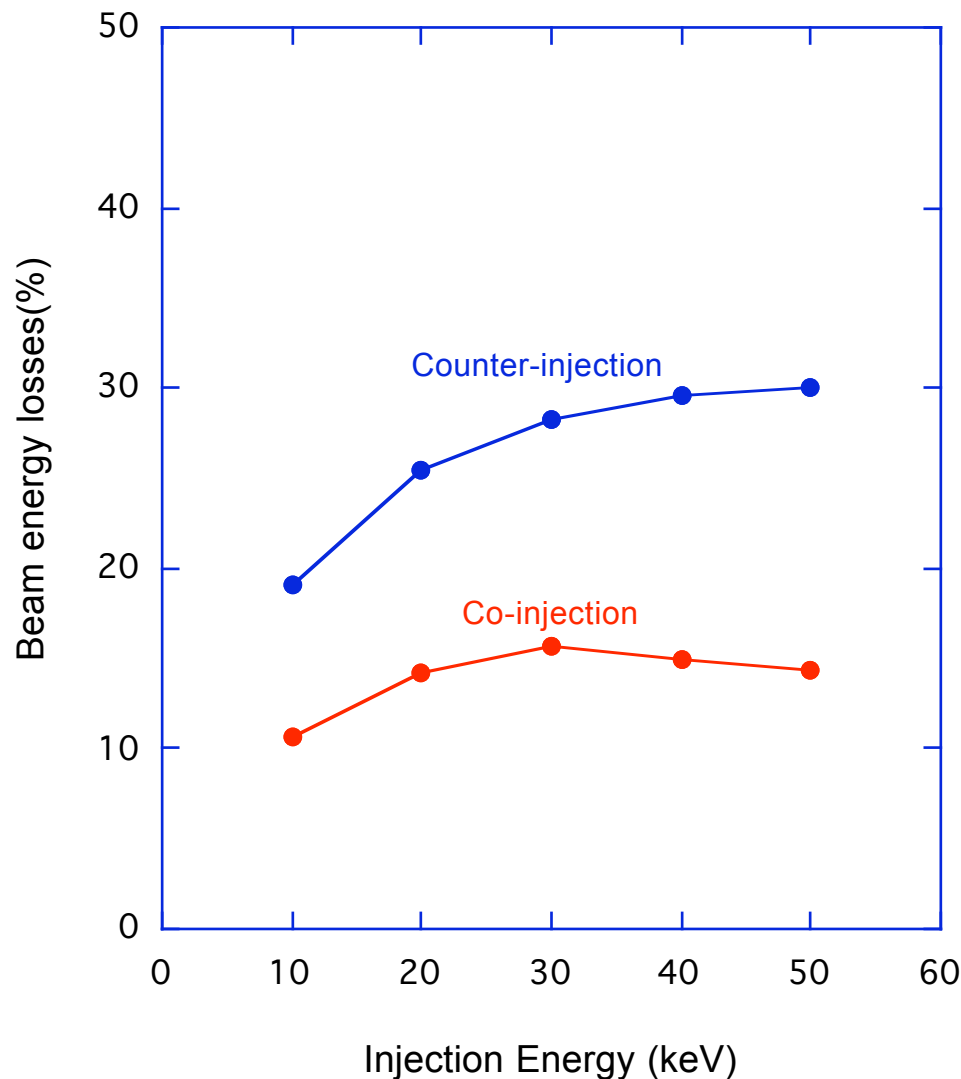
Neutral beam heating efficiency calculations: exit energies and pitch angles



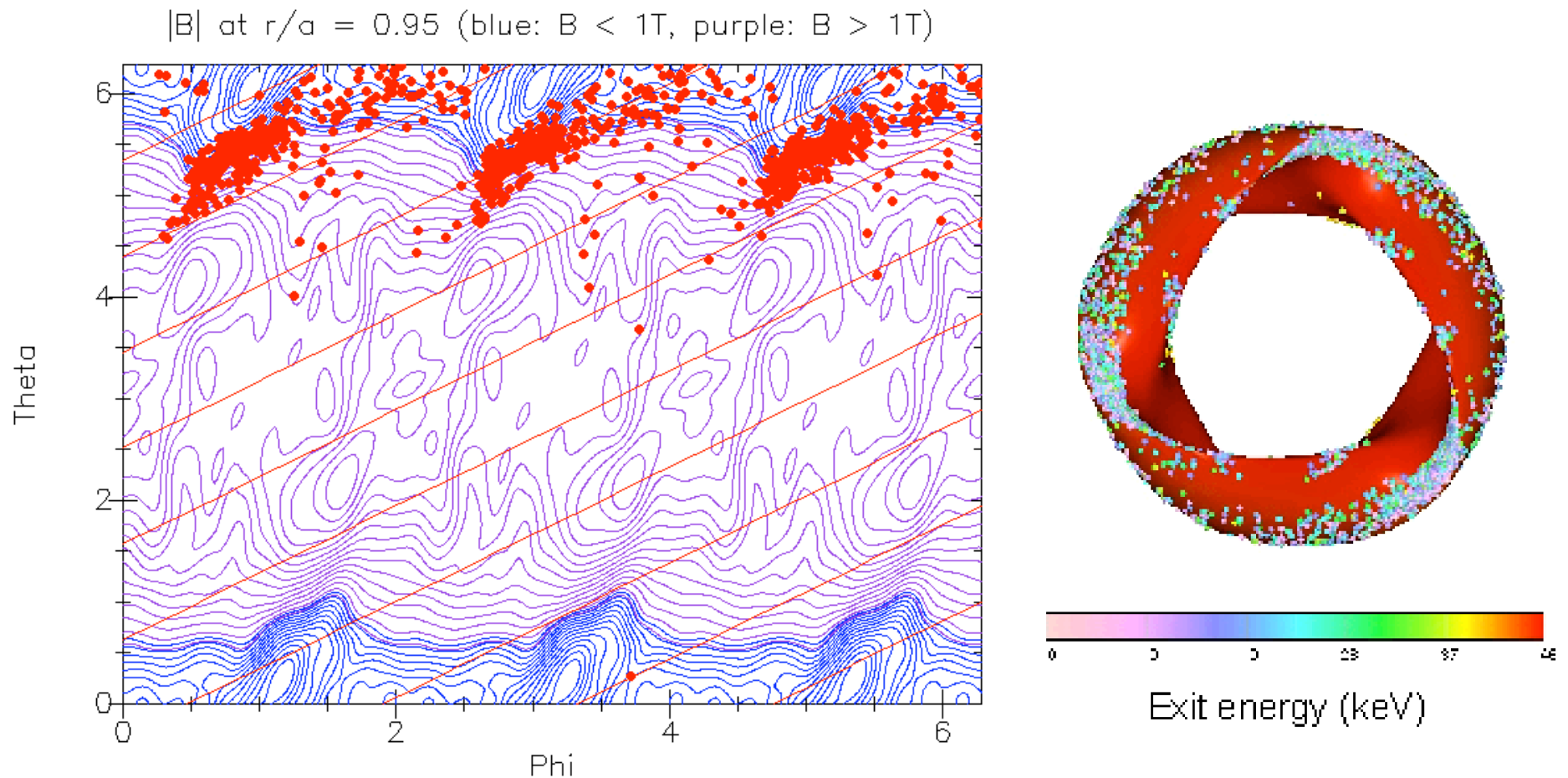
Neutral beam heating efficiency calculations: B and R_{tan} scaling



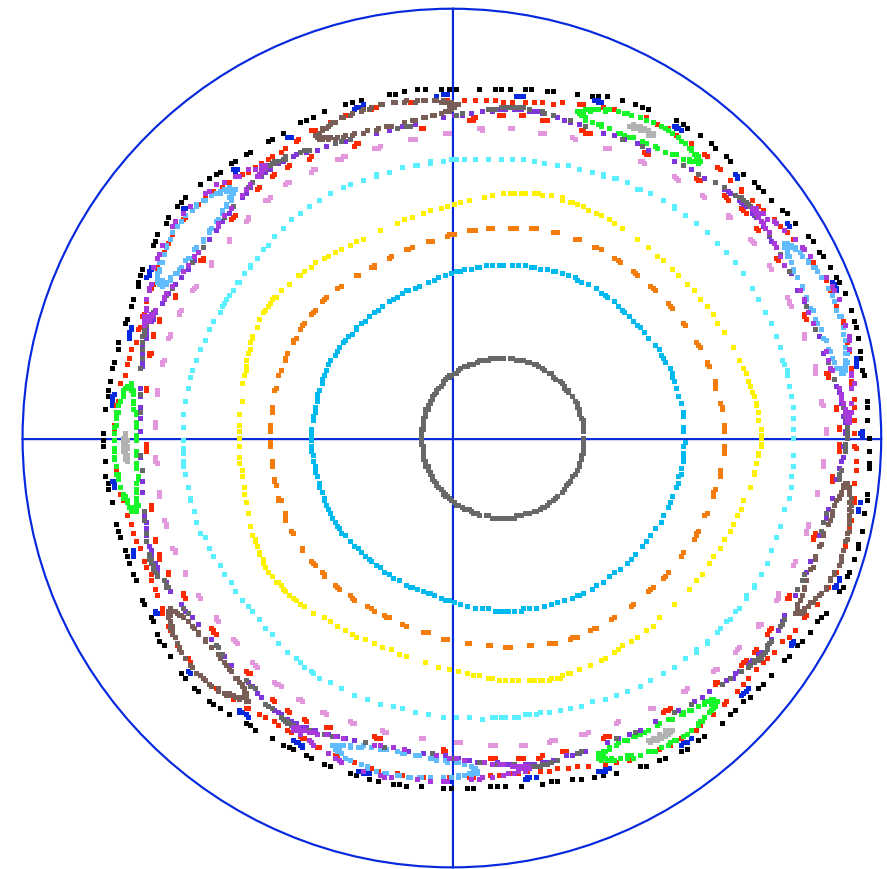
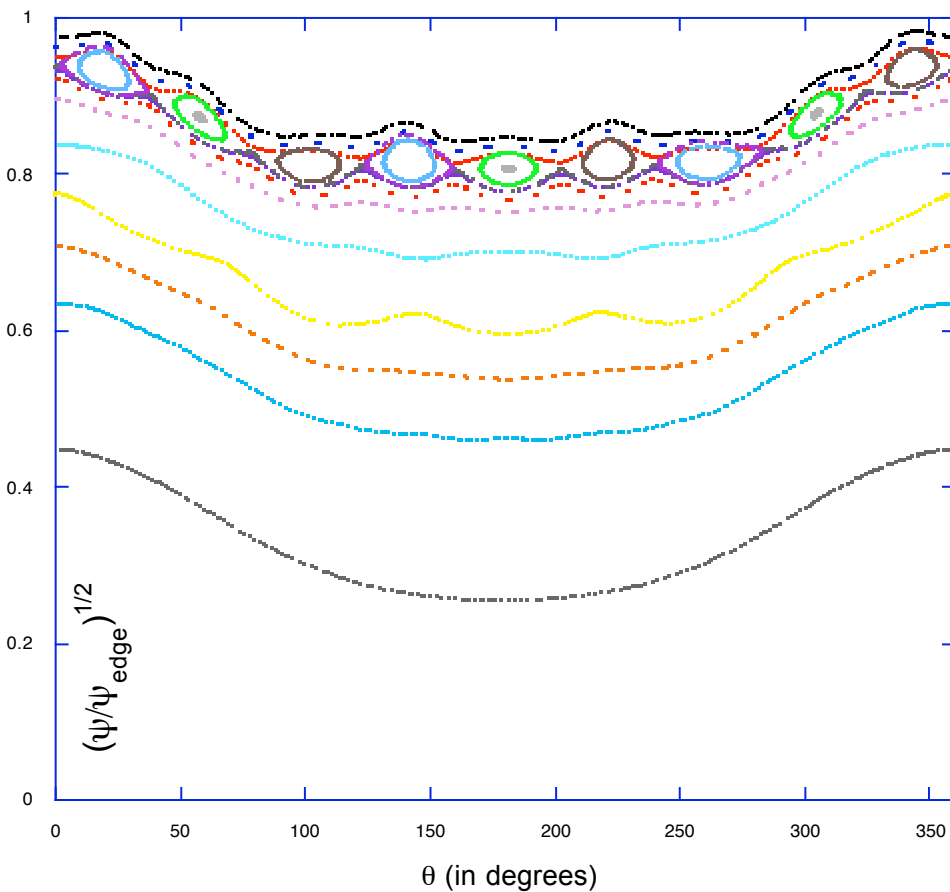
Neutral beam heating efficiency calculations: energy scaling



Neutral beam heating efficiency calculations: loss locations



Drift island structures near edge of QA configuration for energetic (40 keV) passing ions



Conclusions and Future Directions

- QPS has attained low levels of neoclassical transport using a number of confinement based targets:
 - NEO Δ_{eff} , QP-symmetry, DKES plateau regime coefficients
- Flexibility is attained using 7 independently variable coil currents
 - Factor of 40-50 variation in NEO Δ_{eff}
 - Factor of ~10 variation in DKES L_{11} transport coefficient
 - Factor of ~2 variation in Monte Carlo global energy lifetime
- Future efforts will focus on
 - Benchmarking of different calculations for QPS configurations
 - Incorporate neoclassical viscous damping effects into DKES (H. Sugama, S. Nishimura, Phys. Plasmas Nov., 2002)
 - Develop non-diffusive models

New approaches to transport: non-diffusive scaling

- Verification of asymptotic diffusive behavior using tracer particles can be problematical in stellarators due to:
 - Finite system size
 - Convective losses
 - Characteristic step size for some particle classes not \ll system size
- Other approaches: PDF of times at which particles reach a fixed displacement, fractional derivative equations, finite size Lyapunov numbers

